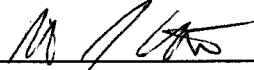
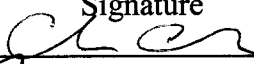


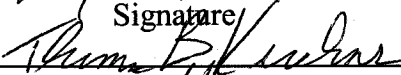

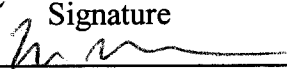
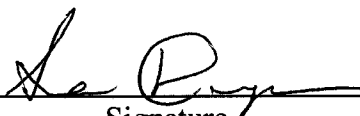

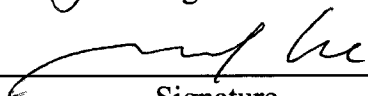


553039

**Sandia National Laboratories
Waste Isolation Pilot Plant**

**Summary Report of the CRA-2009
Performance Assessment Baseline Calculation**

Author:	Daniel J. Clayton (6711)		2/11/10
	Print	Signature	Date
Author:	R. Chris Camphouse (6711)		2/11/10
	Print	Signature	Date
Author:	James W. Garner (6711)		2-11-2010
	Print	Signature	Date
Author:	Ahmed E. Ismail (6711)		2/11/10
	Print	Signature	Date
Author:	Thomas B. Kirchner (6711)		2/4/10
	Print	Signature	Date
Author:	Kristopher. L. Kuhlman (6712)		2/11/10
	Print	Signature	Date
Author:	Martin B. Nemer (6711)		2/11/2010
	Print	Signature	Date
Technical Review:	Sean C. Dunagan (6711)		2/11/2010
	Print	Signature	Date
QA Review:	Mario J. Chavez (6710)		2/11/10
	Print	Signature	Date
Management Review:	Moo Y. Lee (6711)		2/11/2010
	Print	Signature	Date

WIPP:1.2.5:PA:QA-L:549013

Information Only

CONTENTS

Executive Summary5

Executive Summary5

1. Introduction6

2. Updates from CRA-2009 PA to PABC-2009.....7

 2.1 Inventory7

 2.2 Actinide Solubility Limits.....8

 2.3 Culebra Transmissivity Fields8

 2.4 Drilling Parameters9

 2.5 Matrix Partition Coefficients9

 2.6 Input File Reviews9

3. Calculation Methodology11

 3.1 Run Control.....13

 3.2 Parameter Sampling.....13

 3.3 Salado Flow13

 3.4 Salado Transport13

 3.5 Solid Source Term14

 3.6 Direct Solids Release via Cuttings and Cavings.....14

 3.7 Direct Solids Release via Spallings14

 3.8 Actinide Mobilization15

 3.9 Direct Brine Release15

 3.10 Groundwater Flow15

 3.11 Groundwater Transport.....15

 3.12 Normalized Releases.....15

 3.13 Sensitivity Analysis16

4. Results for the Undisturbed Repository17

 4.1 Salado Flow17

 4.1.1 Pressure in the Repository.....17

 4.1.2 Brine Saturation in the Waste.....18

 4.1.3 Brine Flow Out of the Repository19

 4.2 Radionuclide Transport.....21

 4.2.1 Through the Shaft.....21

 4.2.2 Through the Marker Beds21

5. Results for a Disturbed Repository.....22

 5.1 Drilling Scenarios22

 5.2 Mining Scenarios23

 5.3 Salado Flow23

 5.3.1 Pressure in the Repository.....23

 5.3.2 Brine Saturation in the Waste.....25

 5.3.3 Brine Flow Out of the Repository27

Summary Report of the CRA-2009 Performance Assessment Baseline Calculation

5.4 Radionuclide Transport.....30
 5.4.1 Radionuclide Source Term.....31
 5.4.2 Through the Shaft.....32
 5.4.3 Through the Marker Beds32
 5.4.4 Through the Borehole.....33
 5.4.5 Through the Culebra.....35
 5.5 Direct Releases.....37
 5.5.1 Solid Source Term.....37
 5.5.2 Cuttings and Cavings38
 5.5.3 Spallings.....39
 5.5.4 Direct Brine Releases41
 6. Normalized Releases43
 6.1 Cuttings and Cavings43
 6.2 Spallings.....43
 6.3 Direct Brine Releases.....45
 6.4 Groundwater Transport.....46
 6.5 Total46
 References.....50

FIGURES

Figure 3-1. Primary computation models used in the PABC-2009. 12
 Figure 4-1. Pressure in the Waste Panel region, replicate R1, scenario S1, PABC-2009. 18
 Figure 4-2. Brine saturation in the Waste Panel region, replicate R1, scenario S1, PABC-2009. 19
 Figure 4-3. Brine volume flowing away from the repository, replicate R1, scenario S1, PABC-2009..... 20
 Figure 4-4. Brine volume flowing via all MBs across the LWB, replicate R1, scenario S1, PABC-2009..... 20
 Figure 5-1. Pressure in the Waste Panel region, replicate R1, scenario S2, PABC-2009. 24
 Figure 5-2. Pressure in the Waste Panel region, replicate R1, scenario S4, PABC-2009. 24
 Figure 5-3. Brine saturation in the Waste Panel region, replicate R1, scenario S2, PABC-2009. 26
 Figure 5-4. Brine saturation in the Waste Panel region, replicate R1, scenario S4, PABC-2009. 26
 Figure 5-5. Brine volume flowing away from the repository, replicate R1, scenario S2, PABC-2009..... 28
 Figure 5-6. Brine volume flowing via all MBs across the LWB, replicate R1, scenario S2, PABC-2009..... 28
 Figure 5-7. Brine volume flowing away from the repository, replicate R1, scenario S4, PABC-2009..... 29
 Figure 5-8. Brine volume flowing via all MBs across the LWB, replicate R1, scenario S4, PABC-2009..... 30
 Figure 5-9. Total mobilized concentrations in Salado brine, replicate R1, PABC-2009..... 31
 Figure 5-10. Total mobilized concentrations in Castile brine, replicate R1, PABC-2009. 32

Summary Report of the CRA-2009 Performance Assessment Baseline Calculation

Figure 5-11. Cumulative normalized release to the Culebra, scenario S2, PABC-2009. 33

Figure 5-12. Cumulative normalized release to the Culebra, scenario S3, PABC-2009. 34

Figure 5-13. Cumulative normalized release to the Culebra, scenario S4, PABC-2009. 34

Figure 5-14. Cumulative normalized release to the Culebra, scenario S5, PABC-2009. 35

Figure 5-15. Cumulative normalized release to the Culebra, scenario S6, PABC-2009. 35

Figure 5-16. Total and individual normalized radionuclide activity from closure to 10,000 years, PABC-2009. 38

Figure 5-17. Scatter plot of cuttings and cavings areas versus shear strength, PABC-2009. 39

Figure 5-18. Sensitivity of DBR volumes to pressure and mobile brine saturation, replicate R1, scenario S2, Lower panel, PABC-2009. Symbols indicate the range of mobile brine saturation given in the legend. 42

Figure 6-1. Overall mean CCDFs for cuttings and cavings releases in EPA units, PABC-2009 and CRA-2009 PA. 44

Figure 6-2. Overall mean CCDFs for spallings releases in EPA units, PABC-2009 and CRA-2009 PA. 44

Figure 6-3. Overall mean CCDFs for DBRs in EPA units, PABC-2009 and CRA-2009 PA. 45

Figure 6-4. Mean CCDFs for releases from the Culebra in EPA units, PABC-2009 and CRA-2009 PA. 46

Figure 6-5. Confidence interval on overall mean CCDF for total normalized releases in EPA units, PABC-2009. 47

Figure 6-6. Total normalized releases in EPA units, replicates R1, R2 and R3, PABC-2009. 48

Figure 6-7. Overall mean CCDFs for components of total normalized releases in EPA units, PABC-2009. 48

Figure 6-8. Overall mean CCDFs for total normalized releases in EPA units, PABC-2009 and CRA-2009 PA. 49

TABLES

Table 2-1. Inventory parameters modified for the PABC-2009. 8

Table 2-2. Solubility parameters modified for the PABC-2009. 8

Table 2-3. Culebra and Magenta parameters modified for the PABC-2009. 9

Table 2-4. Drilling parameters modified for the PABC-2009. 9

Table 2-5. Matrix partition coefficient ranges modified for the PABC-2009. 9

Table 5-1. WIPP PA modeling scenarios. 23

Table 5-2. PABC-2009 Culebra transport statistics. 36

Table 5-3. PABC-2009 cuttings and cavings area statistics. 38

Table 5-4. PABC-2009 spallings volume statistics. 40

Table 5-5. PABC-2009 DBR volume statistics. 41

Table 6-1. PABC-2009 and CRA-2009 PA statistics on the overall mean for total normalized releases in EPA units at probabilities of 0.1 and 0.001. 49

EXECUTIVE SUMMARY

Containment of transuranic (TRU) waste at the Waste Isolation Pilot Plant (WIPP) is regulated by the U.S. Environmental Protection Agency (EPA) according to the regulations set forth in Title 40 of the Code of Federal Regulations (CFR), Part 191 (U.S. EPA 1993). The U.S. Department of Energy (DOE) demonstrates compliance with the containment requirements according to the Certification Criteria in Title 40 CFR Part 194 (U.S. EPA 1996) by means of performance assessment (PA) calculations. WIPP PA calculations estimate the probability and consequence of potential radionuclide releases from the repository to the accessible environment for a regulatory period of 10,000 years after facility closure. The models are maintained and updated with new information as part of a recertification process that occurs at five-year intervals following receipt in 1999 of the first shipment of waste at the site.

As part of the recertification process, an additional PA calculation, referred to as the 2009 Compliance Recertification Application Performance Assessment Baseline Calculation (PABC-2009) has been conducted. The PABC-2009 demonstrates that the WIPP continues to comply with the containment requirements according to the certification criteria. As required by regulation, results of the PA are displayed as complementary cumulative distribution functions (CCDFs) that display the probability of exceeding various levels of cumulative releases from the disposal system. These CCDFs are calculated using reasonable and, in many cases, conservative conceptual models based on the scientific understanding of the disposal system's behavior. Parameters used in these models are derived from experimental data, field observations, and relevant technical literature.

The overall mean CCDF continues to lie entirely below the specified limits and the WIPP therefore continues to be in compliance with the containment requirements. No releases are predicted to occur at the ground surface in the absence of human intrusion. Sensitivity analyses show that the location of the mean CCDF is dominated by radionuclide releases that could occur on the surface during an inadvertent penetration of the repository by a future drilling operation. Cuttings, cavings and direct brine releases still dominate. The natural and engineered barrier systems of the WIPP provide robust and effective containment of TRU waste even if the repository is penetrated by multiple boreholes.

1. INTRODUCTION

The Waste Isolation Pilot Plant (WIPP), located in southeastern New Mexico, has been developed by the U.S. Department of Energy (DOE) for the geologic (deep underground) disposal of transuranic (TRU) waste. Containment of TRU waste at the WIPP is regulated by the U.S. Environmental Protection Agency (EPA) according to the regulations set forth in Title 40 of the Code of Federal Regulations (CFR), Part 191 (U.S. EPA 1993). The DOE demonstrates compliance with the containment requirements according to the Certification Criteria in Title 40 CFR Part 194 (U.S. EPA 1996) by means of performance assessment (PA) calculations. WIPP PA calculations estimate the probability and consequence of potential radionuclide releases from the repository to the accessible environment for a regulatory period of 10,000 years after facility closure. The models are maintained and updated with new information as part of a recertification process that occurs at five-year intervals following receipt in 1999 of the first shipment of waste at the site.

PA calculations were included in the 1996 Compliance Certification Application (CCA) (U.S. DOE 1996), and in a subsequent Performance Assessment Verification Test (PAVT) (MacKinnon and Freeze 1997a, 1997b and 1997c). Based in part on the CCA and PAVT PA calculations, the EPA certified that the WIPP met the containment criteria in the regulations and was approved for disposal of transuranic waste in May 1998 (U.S. EPA 1998). PA calculations were also an integral part of the 2004 Compliance Recertification Application (CRA-2004) (U.S. DOE 2004). During their review of the CRA-2004, the EPA requested an additional PA calculation, referred to as the CRA-2004 Performance Assessment Baseline Calculation (PABC) (Leigh et al. 2005), be conducted with modified assumptions and parameter values (Cotsworth 2005).

Since the CRA-2004 PABC, additional PA calculations were completed for and documented in the 2009 Compliance Recertification Application (CRA-2009). The CRA-2009 PA resulted from continued review of the CRA-2004 PABC, including a number of technical changes and corrections, as well as updates to parameters and improvements to the PA computer codes (Clayton et al. 2008). The EPA has requested that additional information, which was received between the commencement of the CRA-2009 PA (December 2007) and the submittal of the CRA-2009 (March 2009), be included in an additional PA calculation (Cotsworth 2009), referred to as the CRA-2009 Performance Assessment Baseline Calculation (PABC-2009). The PABC-2009 analysis is guided by AP-145 (Clayton 2009a). This report summarizes the PABC-2009 results.

2. UPDATES FROM CRA-2009 PA TO PABC-2009

PA includes an analysis of the features, events, and processes (FEPs) that may have bearing on the performance of the repository. The FEPs are screened to determine which FEPs are retained in PA. A FEPs impact assessment was conducted according to SP 9-4 (Kirkes 2009c) in support of the PABC-2009 to determine if the changes associated with the PABC-2009 created any inconsistencies or conflicts with the current FEPs baseline. The FEPs impact assessment did not identify any inconsistencies, omissions, or other problems with the current baseline in consideration of the proposed changes for the PABC-2009 (Kirkes 2009b). The assessment concluded that no revision to the baseline FEPs list (Kirkes 2009a) was warranted due to the changes associated with the PABC-2009 (Kirkes 2009b).

Scenarios are formulated from FEPs. The scenarios are modeled using conceptual models that represent the physical and chemical processes of the repository. The scenarios for PABC-2009 and CRA-2009 PA are identical.

The conceptual models are implemented through a series of computer simulations and associated parameters that describe the natural and engineered components of the disposal system (e.g., site characteristics, waste forms, waste quantities, and engineered features). In general, the conceptual models and parameters in the PABC-2009 are the same as the CRA-2009 PA, except the PABC-2009 contains several updates from the CRA-2009 PA. The updates include the inventory, actinide solubilities, Culebra transmissivity fields, drilling parameters, matrix partition coefficients and input file reviews. Nineteen new parameters were created and 130 parameters were modified to account for these updates (Clayton 2010b). The following sections describe how these issues were accounted for in the PABC-2009 and how they differ from the CRA-2009 PA.

2.1 INVENTORY

The Performance Assessment Inventory Report (PAIR)-2008 (Crawford et al. 2009) contains updated estimates for the radionuclide content and waste material parameters, scaled to a full repository, based on information available up to December 31, 2007. The PAIR-2008 also includes information on the volume and radionuclide content for each waste stream. This information is used to generate the probability of encountering a waste stream and the normalized release as a function of time for each waste stream. In order to incorporate this update to the inventory into PA, the parameters for the initial radionuclides, chemical components and waste material inventories were updated (Fox et al. 2009). Furthermore, parameters that are calculated based on the initial radionuclide inventories, such as the Waste Unit Factor (WUF) and the initial lumped radionuclide inventories were updated (Fox et al. 2009). Along with the parameter updates, the analysis of the radionuclides that dominate releases and the solid source term modeling code (EPAUNI) input files were updated (Fox et al. 2009). Table 2-1 lists the inventory parameters that were updated to include the information in the PAIR-2008 (Crawford et al. 2009).

Table 2-1. Inventory parameters modified for the PABC-2009.

Description	Materials	Properties
WIPP-Scale Initial Radionuclide Inventory In Curies	AM241, AM243, CF252, CM243, CM244, CM245, CM248, CS137, NP237, PA231, PB210, PM147, PU238, PU239, PU240, PU241, PU242, PU244, RA226, RA228, SR90, TH229, TH230, TH232, U233, U234, U235, U236, U238	INVCHD and INVRHD
WIPP-Scale Initial Lumped Radionuclide Inventory In Curies	AM241L, TH230L, PU238L, U234L, PU239L	INVCHD and INVRHD
Waste Unit Factor	BOREHOLE	WUF
Waste Stream Information	The volume (in m ³) and radionuclide content (in Curies) of each waste stream (stored in the input files for EPAUNI)	
WIPP-Scale Masses of Nitrate and Sulfate	NITRATE, SULFATE	QINIT
Waste Material Parameters	WAS_AREA	DIRONCHW, DIRONRHW, DIRNCCHW, DIRNCRHW, DCELLCHW, DCELLRHW, DCELCCCHW, DCELECHW, DPLASCHW, DPLASRHW, DPLSCCHW, DPLSCRHW, DPLSECHW, DRUBBCHW, DRUBBRHW

2.2 ACTINIDE SOLUBILITY LIMITS

The solubility limits of the actinide elements are influenced by the chemical components of the waste. With the release of the PAIR-2008 (Crawford et al. 2009), updated information on the amounts of various chemical components in the waste is available. To incorporate this updated information, the parameters for the baseline solubility limits of the actinide elements were updated (Brush et al. 2009). Furthermore, additional experimental results have been published in the literature, which are available to use to enhance the uncertainty distributions for the actinide solubility limits. Using these additional experimental results, the solubility limit uncertainty distribution has been updated (Xiong et al. 2009). Table 2-2 lists the solubility limit parameters that were updated to include this additional information.

Table 2-2. Solubility parameters modified for the PABC-2009.

Description	Materials	Properties
Actinide Solubilities in Castile and Salado Brines	SOLMOD3, SOLMOD4	SOLCOH, SOLSOH, SOLVAR
	SOLMOD5	SOLCOH, SOLSOH

2.3 CULEBRA TRANSMISSIVITY FIELDS

A peer review panel evaluated changes in the conceptual model to relate the Culebra transmissivity to various geologic factors; the changes to the model were subsequently approved (Burgess et al. 2008). The additional data sets and modified conceptual model were used for the PABC-2009 transmissivity fields (T-fields) calibration. Furthermore, the additional data sets were used to calculate parameters used to represent the Culebra and Magenta properties in the Salado flow calculations (Beauheim 2009). Table 2-3 lists the Culebra and Magenta parameters that were updated to include this information.

Table 2-3. Culebra and Magenta parameters modified for the PABC-2009.

Description	Materials	Properties
Brine far-field pore pressure	CULEBRA, MAGENTA	PRESSURE
Log of intrinsic permeability	CULEBRA, MAGENTA	PRMX_LOG, PRMY_LOG, PRMZ_LOG

2.4 DRILLING PARAMETERS

The WIPP regulations require that current drilling practices should be assumed for future inadvertent intrusions. The DOE continues to survey drilling activity in the Delaware Basin in accordance with the criteria established in 40 CFR 194.33. Local well operators are surveyed annually to provide the WIPP project with information on drilling practices, Castile brine encounters, etc. and the results are documented in the Delaware Basin Monitoring Annual Report (U.S. DOE 2008). The report shows that drilling practices have not changed since the summary report used for the CRA-2009 PA (U.S. DOE 2007). The drilling parameters were updated for the PABC-2009 (Clayton 2009a). Table 2-4 lists the drilling parameters that were updated to include this information.

Table 2-4. Drilling parameters modified for the PABC-2009.

Description	Materials	Properties
Drilling rate per unit area	GLOBAL	LAMBDA_D
Plugging pattern probabilities	GLOBAL	ONEPLG, TWOPLG, THREEPLG

2.5 MATRIX PARTITION COEFFICIENTS

As noted in the third set of the EPA's completeness comments (Kelly, 2009), comment 3-C-25, the matrix partition coefficient (K_d) values used in the CRA-2009 PA were derived from experimental data with low organic ligand concentrations (Brush and Storz 1996). Based on the information in the PAIR-2008 (Crawford et al. 2009), the predicted organic ligand concentrations have increased significantly. The EPA recommended that the K_d ranges be revisited based on the higher organic ligand concentrations (Kelly, 2009). The K_d ranges were updated to account for the higher organic ligand concentrations for the PABC-2009 (Clayton 2009e). Table 2-5 lists the K_d ranges that were updated to include this information.

Table 2-5. Matrix partition coefficient ranges modified for the PABC-2009.

Description	Materials	Properties
Matrix Partition Coefficient for Americium	AM+3	MKD_AM
Matrix Partition Coefficient for Neptunium	NP+4	MKD_NP
Matrix Partition Coefficient for Neptunium	NP+5	MKD_NP
Matrix Partition Coefficient for Plutonium	PU+3	MKD_PU
Matrix Partition Coefficient for Plutonium	PU+4	MKD_PU
Matrix Partition Coefficient for Thorium	TH+4	MKD_TH
Matrix Partition Coefficient for Uranium	U+4	MKD_U

2.6 INPUT FILE REVIEWS

A review of the input files was conducted before the commencement of the PABC-2009 (Chavez 2009). One of the review aspects was to ensure that the input files reference the correct parameter from the parameter database versus having a numerical value typed in the input files and if appropriate, a new parameter is created in the parameter database to capture the numerical

Summary Report of the CRA-2009 Performance Assessment Baseline Calculation

value in the input file. Parameters from the parameter database are conveyed into the calculations via a preprocessing step. The input files for the subsequent preprocessors and codes can then use these parameters to calculate derived parameters. Ensuring that the calculations are based on values in the parameter database will help to maintain consistency.

As a result of the input file review:

1. Nineteen parameters were added to the parameter database (Clayton 2009a, Clayton 2009d and Nemer 2009).
2. Seventeen parameters were modified so that the value in the parameter database matches the value used in the analyses (Nemer 2009).
3. The grid used for DBR was updated to increase consistency between the BRAGFLO and DBR grids (Clayton 2010a).
4. The run sequences for the NUTS and PANEL calculations were updated to remove the numerical values typed in the input files (Clayton 2009c, Ismail and Garner 2010).
5. Unnecessary calculations were removed from several input files (Clayton 2010a, Ismail and Garner 2010, Nemer 2009).
6. The number of input files needed for the NUTS and DBR calculations was reduced (Clayton 2009b, Ismail and Garner 2010).
7. An error in a DBR input file was corrected (Clayton 2009b).

These changes had little to no effect on the results, but were implemented to increase consistency. Their inclusion in the PABC-2009 should reduce possible future errors as well.

3. CALCULATION METHODOLOGY

The WIPP PA quantifies the potential releases of radioactive materials from the disposal system to the accessible environment over the 10,000-year regulatory period using a suite of numerical models. These numerical models are implemented in various computer codes as shown in Figure 3-1. There is a significant amount of uncertainty associated with characterizing the physical properties of geologic materials that influence potential releases. WIPP PA considers both subjective (epistemic) uncertainty and stochastic (aleatory) uncertainty.

Properties such as permeability and porosity are usually measured indirectly and can vary significantly depending upon location. This uncertainty in the appropriate value to assign to certain physical properties is termed subjective uncertainty. Subjective uncertainty can, in theory, be reduced by further study of the system. Subjective uncertainty is dealt with in WIPP PA by running multiple realizations in which the values of uncertain parameters are varied.

There is uncertainty in predicting what will happen near the WIPP in the future. The uncertainty in future events is termed stochastic uncertainty. Unlike subjective uncertainty, stochastic uncertainty cannot be reduced by further study. Stochastic uncertainty is dealt with in WIPP PA by determining multiple possible sequences of future events and analyzing the outcomes for each one.

To ensure that parameters are sampled across their full ranges of uncertainty, Latin Hypercube Sampling (LHS) is used to create the realizations. For the WIPP PA, the LHS code (Vugrin 2006d) is used to create a “replicate” of 100 distinct parameter sets (“vectors”) that span a wide range of parameter uncertainty. Three replicates are run for a total of 300 separate vectors to ensure that the Latin hypercube replicates are representative. This is the start of the WIPP PA calculation.

For each of the 300 vectors, several codes are run. The BRAGFLO code (Nemer 2007) is used to calculate Salado brine and gas flow. The NUTS code (Gilkey 2006) is used to calculate Salado radionuclide transport. The EPAUNI code (Leigh 2006) determines the normalized solid source term for use with the direct solid releases. The CUTTINGS_S code (Vugrin 2006a) is used to calculate direct solids releases via cuttings and cavings. The DRSPALL code (Vugrin 2006b) and the CUTTINGS_S code are used to calculate direct solids releases via spallings. The PANEL code (Garner 2006) quantifies the mobilization of actinides by brine. The BRAGFLO code is used to calculate direct brine release volumes. The MODFLOW 2000 code (McKenna and Chavez 2005) is used to calculate brine flow in the Culebra, while the SECOTP2D code (Kanney 2006) is used to calculate radionuclide transport in the Culebra. All of these calculations address the subjective uncertainty by producing results for the 300 separate vectors.

To deal with stochastic uncertainty, WIPP PA employs a standard Monte Carlo method of sampling on random “futures.” A future is defined as one possible sequence of events. The CCDFGF code (Vugrin 2006c) uses the results from the other codes to construct individual futures and ultimately, CCDFs. The sensitivities of the CCDFs to the sampled input parameters are determined using the STEPWISE code (Kirchner 2006) by performing a multiple regression analysis.

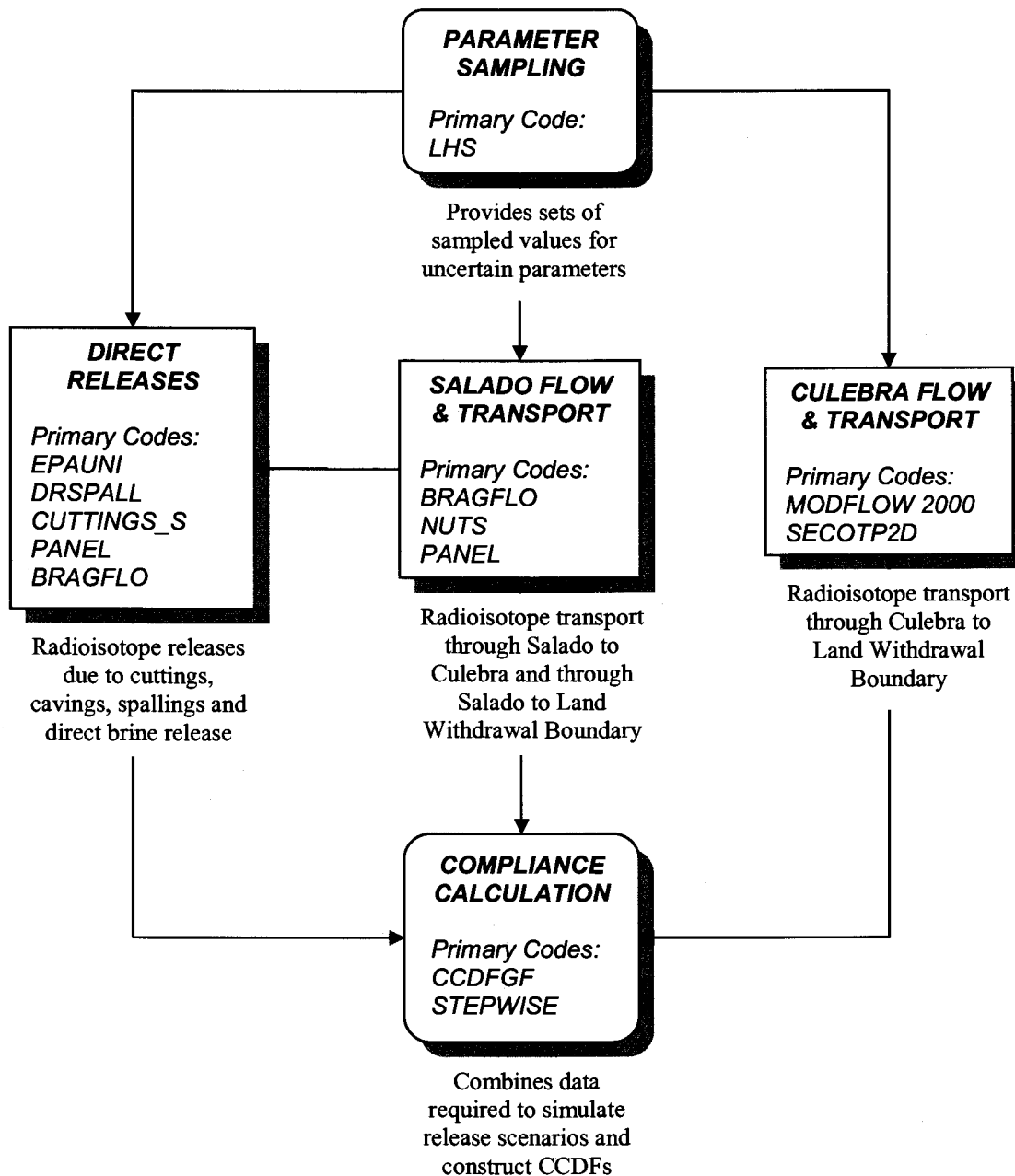


Figure 3-1. Primary computation models used in the PABC-2009.

This section provides a summary of the PA calculations for the PABC-2009. For each of the processes discussed above, an individual analysis package has been produced. The analysis package gives details of the calculation, describes the changes that were made to produce the PABC-2009, and gives a comparison between the PABC-2009 and the CRA-2009 PA. A description of each analysis and references to the analysis packages are provided in the following sections.

3.1 RUN CONTROL

Digital Command Language (DCL) scripts, referred to here as EVAL run scripts, are used to implement and document the running of all software. These scripts, which are the basis for the WIPP PA run control system, are stored in the LIBPABC09_EVAL Code Management System (CMS) library. All inputs are fetched at run time by the scripts, and outputs and run logs are automatically stored by the scripts in the CMS libraries. Run control for the PABC-2009 calculations is documented in Long (2010).

3.2 PARAMETER SAMPLING

The primary role of the code LHS (Vugrin 2006d) is to use Latin hypercube sampling to sample the subjectively uncertain parameters used in WIPP PA. Additionally, LHS uses these sampled parameters to create the 100 vectors per replicate that are input into the suite of codes used in WIPP PA. An analysis of PABC-2009 LHS calculations and a comparison to the CRA-2009 PA are provided in the LHS analysis package (Kirchner 2010a). LHS version 2.42 was used for both the PABC-2009 and the CRA-2009 PA.

3.3 SALADO FLOW

The code BRAGFLO (Nemer 2007) simulates brine and gas flow in and around the repository. BRAGFLO includes the effects of processes such as gas generation and creep closure. Outputs from the BRAGFLO simulations describe the conditions (pressure, brine saturation, porosity) and flow patterns (brine flow up an intrusion borehole and out anhydrite marker beds to the accessible environment) that are used by other software to predict radionuclide releases. Analysis of the PABC-2009 BRAGFLO calculations and a comparison to the CRA-2009 PA are provided in the BRAGFLO analysis package (Nemer 2010). BRAGFLO version 6.0 was used for both the PABC-2009 and the CRA-2009 PA.

3.4 SALADO TRANSPORT

The radionuclide transport code NUTS (Gilkey 2006) simulates the transport of radionuclides through the Salado Formation for the single intrusion scenarios. Two types of NUTS runs are made for PA calculations. "Screening" runs use a conservative tracer to determine which vector/scenario combinations have potential for radionuclides to reach the accessible environment. These vector/scenario combinations are included in "isotope" and "time intrusion" runs which calculate the transport of actual radionuclides. Analysis of the PABC-2009 NUTS calculations, including a comparison to the CRA-2009 PA, is provided in the NUTS analysis package (Ismail and Garner 2010). NUTS version 2.05c was used for both the PABC-2009 and the CRA-2009 PA.

Radionuclide transport to the Culebra for the multiple intrusion scenario is calculated by running the PANEL code (Garner 2006) in "intrusion mode" (PANEL_INT). Analysis of the PABC-2009 PANEL_INT calculations, including a comparison to the CRA-2009 PA, is provided in the NUTS analysis package (Ismail and Garner 2010). PANEL version 4.03 was used for both the PABC-2009 and the CRA-2009 PA.

3.5 SOLID SOURCE TERM

The EPAUNI code (Leigh 2006) calculates the decay of the radionuclide components in each inventory waste stream over the 10,000-year regulatory period (for use in calculating direct solids releases, see Sections 3.6 and 3.7). These calculations are deterministic, so multiple replicates and vectors of uncertain parameters are not used. Calculations are performed for both contact-handled (CH) and remote-handled (RH) waste. None of the changes made for the CRA-2009 PA affected the solid source term calculations, so the CRA-2004 PABC EPAUNI calculations were used in the CRA-2009 PA. Solid source term calculations were performed as part of the PABC-2009. An analysis of the PABC-2009 EPAUNI calculations, including a comparison to the CRA-2004 PABC, is provided in the EPAUNI analysis package (Fox and Clayton 2010). EPAUNI version 1.15A was used for both the PABC-2009 and the CRA-2004 PABC.

3.6 DIRECT SOLIDS RELEASE VIA CUTTINGS AND CAVINGS

Cuttings and cavings are the solid material removed from the repository and carried to the surface by the drilling fluid during the process of drilling a borehole. Cuttings are the materials removed directly by the drill bit, and cavings are the material eroded from the walls of the borehole by shear stresses from the circulating drill fluid. The CUTTINGS_S code (Vugrin 2006a) calculates the quantity of material brought to the surface from a radioactive waste disposal repository as a consequence of an inadvertent human intrusion through drilling. WIPP PA utilizes the code CUTTINGS_S to calculate the amount of material removed from the repository by cuttings and cavings. Analysis of the PABC-2009 CUTTINGS_S calculations and a comparison to the CRA-2009 PA are provided in the CUTTINGS_S analysis package (Ismail 2010). CUTTINGS_S version 6.02 was used for both the PABC-2009 and the CRA-2009 PA.

3.7 DIRECT SOLIDS RELEASE VIA SPALLINGS

A spallings event is a special case of drilling intrusion in which the repository contains gas at high pressure. This highly pressurized gas can cause localized mechanical failure and entrainment of solid waste into and up the borehole, resulting in transport to the land surface. The computer code DRSPALL (Vugrin 2006b) was developed to calculate the spallings volume from a single borehole intrusion. None of the changes incorporated in the PABC-2009 or CRA-2009 PA affected the DRSPALL calculations, so the CRA-2004 PABC DRSPALL calculations were used for the PABC-2009. Analysis of the CRA-2004 PABC DRSPALL calculations is provided in the DRSPALL analysis package (Vugrin 2005). DRSPALL version 1.10 was used in the CRA-2004 PABC.

The CUTTINGS_S code (Vugrin 2006a) uses the repository pressures calculated by BRAGFLO to interpolate spallings volumes from DRSPALL and calculate spallings volumes from an individual intrusion for the various drilling scenarios). Analysis of the PABC-2009 CUTTINGS_S calculations, including a comparison to the CRA-2009 PA, is provided in the CUTTINGS_S analysis package (Ismail 2010). CUTTINGS_S version 6.02 was used for both the PABC-2009 and the CRA-2009 PA.

3.8 ACTINIDE MOBILIZATION

The code PANEL (Garner 2006) has four roles in the WIPP PA system. The first is to compute the potential for actinide mobilization due to dissolution and colloid mobilization, which is the amount of radionuclides mobilized for removal via a brine pathway. The second purpose is to calculate radionuclide decay, and the third is to calculate the amounts of radionuclides mobilized in a panel that contains a given volume of brine. The fourth is to compute the amounts of radionuclides removed by a volume of brine moving up the borehole to the Culebra (see Section 3.4). None of the changes made for the CRA-2009 PA affected the actinide mobilization calculations, so the CRA-2004 PABC PANEL calculations were used in the CRA-2009 PA. Actinide mobilization calculations were performed as part of the PABC-2009. An analysis of the PABC-2009 PANEL calculations, including a comparison to the CRA-2004 PABC, is provided in the PANEL analysis package (Garner 2010). PANEL version 4.03 was used for both the PABC-2009 and the CRA-2004 PABC.

3.9 DIRECT BRINE RELEASE

Direct brine releases (DBRs) are releases of contaminated brine originating in the repository and flowing up an intrusion borehole during the period of drilling. DBR volumes are calculated using the code BRAGFLO (Nemer 2007) with a two-dimensional, horizontally oriented grid, which represents the vicinity of the waste panels. Analysis of the PABC-2009 DBR calculations and a comparison to the CRA-2009 PA are provided in the DBR analysis package (Clayton 2010a). BRAGFLO version 6.0 was used for both the PABC-2009 and the CRA-2009 PA.

3.10 GROUNDWATER FLOW

Flow through the Culebra is calculated by the code MODFLOW 2000 (McKenna and Chavez 2005). None of the changes made for the CRA-2009 PA affected the groundwater flow calculations, so the CRA-2004 PABC MODFLOW 2000 calculations were used in the CRA-2009 PA. Groundwater flow calculations were performed as part of the PABC-2009. Analysis of the PABC-2009 Culebra flow calculations, including a comparison to the CRA-2004 PABC are provided in Kuhlman (2010). MODFLOW 2000 version 1.6 was used for both the PABC-2009 and the CRA-2004 PABC.

3.11 GROUNDWATER TRANSPORT

The code SECOTP2D (Kanney 2006) computes the transport of radionuclides that may be released into the Culebra. None of the changes made for the CRA-2009 PA affected the groundwater transport calculations, so the CRA-2004 PABC SECOTP2D calculations were used in the CRA-2009 PA. Groundwater transport calculations were performed as part of the PABC-2009. Analysis of the PABC-2009 Culebra transport calculations, including a comparison to the CRA-2004 PABC are provided in Kuhlman (2010). SECOTP2D version 1.41a was used for both the PABC-2009 and the CRA-2004 PABC.

3.12 NORMALIZED RELEASES

WIPP PA uses the code CCDFGF (Vugrin 2006c) to address stochastic uncertainty. CCDFGF employs a standard Monte Carlo method of sampling on random "futures". A future is defined

as one possible sequence of events, and each future is based on sampled stochastic variables such as the time and location of a drilling event, plugging pattern used for a drilling event, and whether or not waste was encountered. The CCDFGF code combines the sampled stochastic parameters with the release data calculated by the process model codes to calculate the cumulative normalized release for each future. Using these futures and ordered statistics, CCDFs are created, and these CCDFs are compared to regulatory limits to determine compliance with the EPA regulations. Analysis of the PABC-2009 CCDFGF calculations and a comparison to the CRA-2009 PA are provided in the CCDFGF analysis package (Camphouse 2010). CCDFGF version 5.02 was used for both the PABC-2009 and the CRA-2009 PA.

3.13 SENSITIVITY ANALYSIS

Rank regression analysis was used to evaluate the sensitivity of the output variables to the sampled parameters. The rank regression analyses were conducted using the computer code STEPWISE (Kirchner 2006). STEPWISE relates the sampled input parameter values to the calculated release data by performing a multiple regression analysis and reporting the results in tabular form. Analysis of the PABC-2009 STEPWISE calculations is provided in Kirchner (2010b). STEPWISE version 2.21 was used for both the PABC-2009 and the CRA-2009 PA.

4. RESULTS FOR THE UNDISTURBED REPOSITORY

The PA tabulates releases from the repository for undisturbed conditions. Releases to the accessible environment from the undisturbed repository fall under two sets of protection requirements. The first, as set forth 40 CFR § 191.15, protects individuals from radiological exposure; the second, in 40 CFR § Part 191, Subpart C, protects groundwater resources from contamination. This section shows how WIPP complies with these two requirements by presenting flow and radionuclide transport results from modeling the undisturbed repository.

4.1 SALADO FLOW

This section summarizes the Salado flow calculation results for the undisturbed (S1) scenario. Pressure in the repository, brine saturation in the waste, and brine flow out of the repository are presented, along with sensitivity analyses that identify the uncertain parameters to which these results are most sensitive. The analysis package for Salado flow contains a detailed presentation on the BRAGFLO model, calculation results, and further sensitivity analyses (Nemer 2010).

4.1.1 Pressure in the Repository

In undisturbed conditions, pressure strongly influences the extent to which contaminated brine might migrate from the repository to the accessible environment. In addition, pressure developed under undisturbed conditions is an initial condition for the models for spallings and DBR (Section 5.5.3 and Section 5.5.4 respectively).

Figure 4-1 shows the pressure in the Waste Panel region for 100 vectors in replicate R1, scenario S1 for the PABC-2009. During the first 1,000 years, repository pressure may increase rapidly due to several factors: rapid initial creep closure of rooms, initial inflow of brine causing gas generation due to corrosion; and availability of cellulose, plastic and rubber (CPR) material to produce gas by microbial degradation. Pressure generally approaches a steady-state value after 2,000 years as room closure ceases and brine inflow slows, thereby reducing the amount of gas generated by corrosion and CPR consumption.

Sensitivity analyses are used to determine the importance of parameter uncertainty to the uncertainty in model results. The uncertainty in the pressure in the waste panel is primarily and positively correlated to the sampled input parameter for the halite porosity. The positive correlation indicates that higher pressures result from higher values of halite porosity. Increases in halite porosity increase the volume of brine available in the material overlying the waste, which as the brine flows; can then increase the amount of brine in the repository (Nemer 2010). Microbial gas generation rates are a function of the brine in the repository and increase as more brine is available. Increasing the amount of gas generated results in increased repository pressures.

Overall, pressures are slightly less for the PABC-2009 compared with the CRA-2009 PA (Nemer 2010, Table 6-10). The updated inventory contains a lower amount of CPR, which decreases the amount of gas generated from microbial degradation and in turn decreases pressures. This will decrease spallings and DBR volumes for the first intrusion.

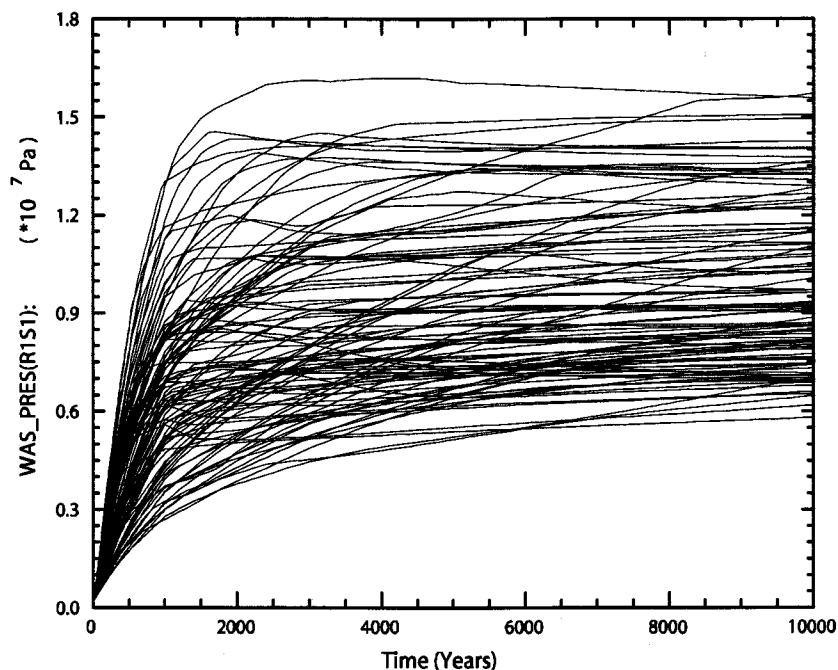


Figure 4-1. Pressure in the Waste Panel region, replicate R1, scenario S1, PABC-2009.

4.1.2 Brine Saturation in the Waste

Brine saturation is an important result of the model for Salado flow because gas generation processes, which tend to increase pressure, require brine. Brine saturation is also an initial condition in the model for DBR (Section 5.5.4).

Figure 4-2 shows brine saturation in the Waste Panel region of the repository for 100 vectors of replicate R1, scenario S1 for the PABC-2009. Brine saturation in the waste-filled areas is set initially to 0.015. Saturation increases very rapidly (in the first 100 years) in all excavated areas as brine flows toward the excavations, primarily from the DRZ above the excavation. Initially there is a large pressure differential between the DRZ and the excavated regions, and the relatively high permeability of the DRZ, compared to undisturbed halite, permit the rapid influx of brine. Brine inflow slows as the pressures equalize and as brine saturation in the DRZ decreases. Brine saturation in the waste areas decreases over time as brine is consumed by corrosion. Brine may also be driven out of the repository by high pressure.

The uncertainty in brine saturation in the waste panel is dependent on five parameters. The relative importance of these parameters varies over the 10,000-year modeling period, and none of the parameters are clearly dominant. Brine saturation is positively correlated with anhydrite permeability, DRZ permeability, and halite porosity. Increases in halite porosity increase the volume of brine available in the material overlying the waste; increases in DRZ and anhydrite permeability accelerate brine flow into the waste. Negative correlations are found between brine saturation and the corrosion rate and the wicking factor because increases in these two variables, increase the rate at which brine is consumed by corrosion, thus decreasing saturation (Nemer 2010).

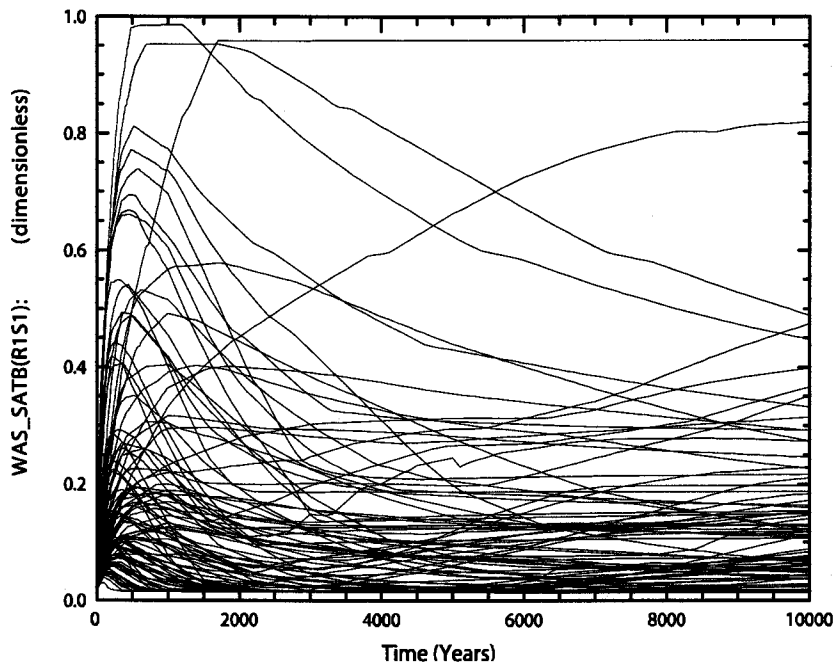


Figure 4-2. Brine saturation in the Waste Panel region, replicate R1, scenario S1, PABC-2009.

Overall, brine saturations for the PABC-2009 are similar to the CRA-2009 PA (Nemer 2010, Table 6-6, 6-7 and 6-8). The updates for the PABC-2009 did not appreciably affect the brine saturation results. This will translate to a negligible change in DBR volumes for the first intrusion.

4.1.3 Brine Flow Out of the Repository

The anhydrite marker beds (MBs) and the shafts provide possible pathways for brine flow away from the repository in the undisturbed (S1) scenario. The Salado flow model only tabulates the volume of brine crossing boundaries within the model grid; it does not identify whether the brine contains radionuclides from the waste. Radionuclide transport is calculated separately from the flow and is discussed in Section 4.2.

Figure 4-3 shows cumulative volume of brine outflow from the waste-filled regions of the repository (BRNREPOC), while Figure 4-4 shows the volumes of brine that cross the Land Withdrawal Boundary (LWB) through the MBs (BRAALLWC). The largest outflow volume across the LWB is $\sim 1,360 \text{ m}^3$. Brine crossing the LWB or moving up the shaft does not necessarily indicate releases from the repository, since the brine may not have been in contact with the waste; the brine may have been present in the MBs at the start of the regulatory period. Section 4.2 presents the results of the radionuclide transport calculations that determine the amount of radionuclides that may be released by transport in brine.

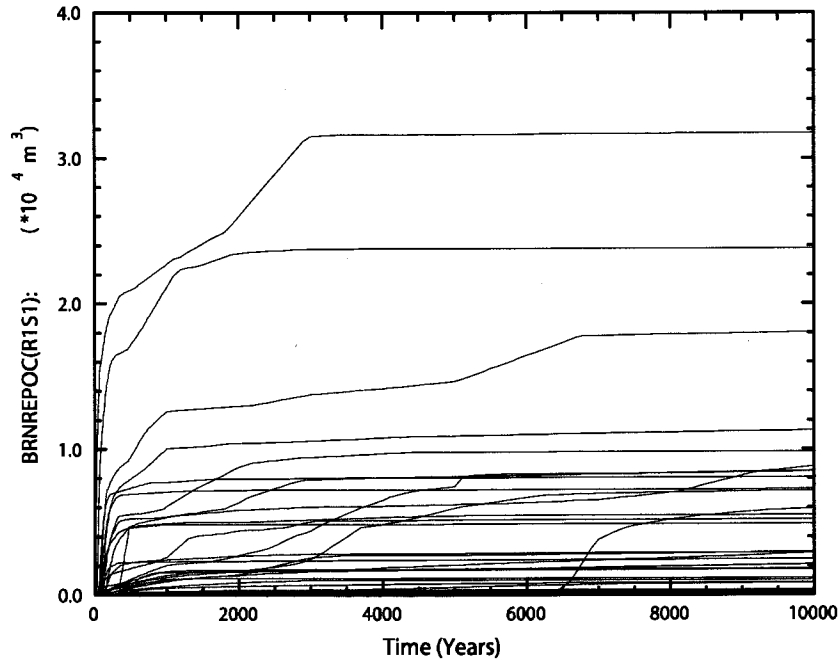


Figure 4-3. Brine volume flowing away from the repository, replicate R1, scenario S1, PABC-2009.

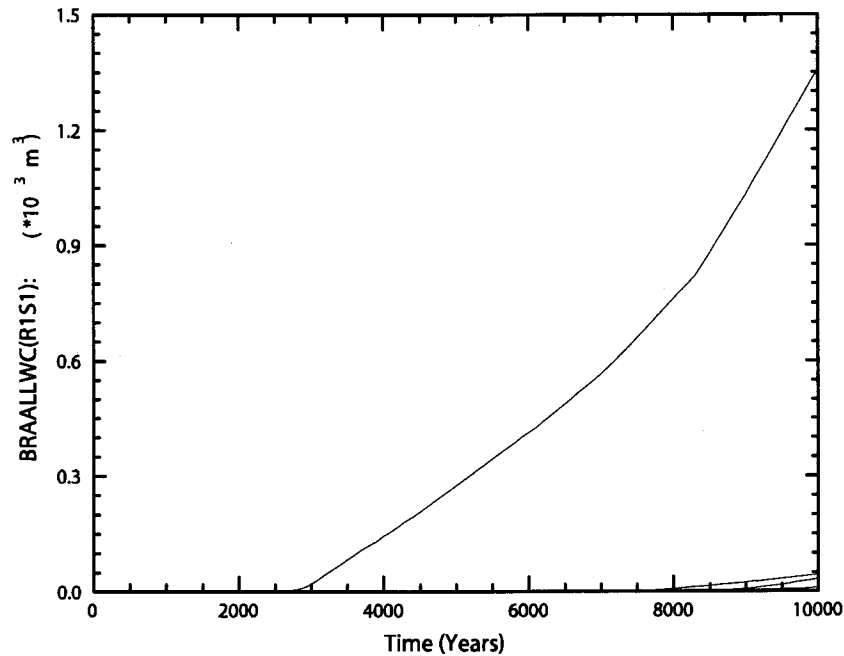


Figure 4-4. Brine volume flowing via all MBs across the LWB, replicate R1, scenario S1, PABC-2009.

Regression analyses between total cumulative brine volume flowing out of the waste-filled regions (BRNREPOC) and the uncertain parameters show that the permeability of the DRZ has the largest positive correlation, followed by the permeability of the concrete panel seal, and the porosity of undisturbed halite. Increases in the permeability of the DRZ and the concrete panel

seal allow more brine to flow out of the repository, as well as into the repository, which increases the amount of gas generated and therefore the pressure. The increase in the halite porosity also increases the pressure (see Section 4.1.1), and an increase in pressure increases the amount of brine flow out of the repository. The largest negative correlation is with the waste residual brine saturation, which determines the immobile portion of the brine in the waste-filled regions, which then limits the amount of brine that can flow out of the repository (Nemer 2010).

Compared with the CRA-2009 PA, the average and maximum cumulative brine volume flowing away from the repository did not change for the PABC-2009 (Nemer 2010, Table 6-11). The change in pressure was not enough to affect total brine flow out of the repository. The cumulative brine volume to the LWB through the MBs decreased for the PABC-2009 compared with the CRA-2009 PA (Nemer 2010, Table 6-12), most likely because of the pressure decrease (see Section 4.1.1).

4.2 RADIONUCLIDE TRANSPORT

This section summarizes the radionuclide transport results for the undisturbed repository, both up the shaft to the Culebra, and through the Salado to the LWB. Ismail and Garner (2010) present a detailed analysis of the NUTS results for the PABC-2009.

Radionuclide transport in the undisturbed (S1) scenario is calculated by the code NUTS. Screening runs using a conservative tracer are conducted to determine which vectors have the potential to transport radionuclides to the accessible environment. Full transport simulations are then performed for all vectors that are screened in (have the potential to transport radionuclides to the accessible environment). Based upon results of the screening exercise, full radionuclide transport simulations were needed for only one vector in the undisturbed case, replicate R1, vector 53.

4.2.1 Through the Shaft

For the undisturbed repository, no vectors showed radionuclide transport through the shafts to the Culebra. Consequently, no radionuclides could be transported through the Culebra to the accessible environment under undisturbed conditions (Ismail and Garner 2010).

4.2.2 Through the Marker Beds

Radionuclides can potentially also be transported through the Salado marker beds to the LWB. For the undisturbed case, only one vector in the PABC-2009 was screened in. The maximum total integrated activity across the LWB at the Salado marker beds for replicate R1, scenario S1, vector 53 was 6.3×10^{-11} EPA units (Ismail and Garner 2010). This is less than the CRA-2009 PA results, which had 2.6×10^{-10} EPA units at the boundary (Ismail and Garner 2008). The releases from the undisturbed scenario are insignificant when compared to releases from drilling intrusions (see Section 5.4). Consequently, releases in the undisturbed (S1) scenario are omitted from the calculation of total releases from the repository. The statutory requirements of 40 CFR 194.55 require that the maximum total radioactivity level for ^{226}Ra and ^{228}Ra in any underground source of drinking water for 10,000 years after disposal be determined and compared to the limit of 5 pCi/L. For the PABC-2009, the maximum concentration is 0.0006 pCi/L, which is well below the limit (Ismail and Garner 2010).

5. RESULTS FOR A DISTURBED REPOSITORY

The WIPP repository might be disturbed by exploratory drilling for natural resources during the 10,000-year regulatory period. Drilling could create additional pathways for radionuclide transport, especially in the Culebra, and could release material directly to the surface. In addition, mining for potash within the LWB might alter flow in the overlying geologic units and may locally accelerate transport through the Culebra. The disturbed scenarios used in PA modeling capture the range of possible releases resulting from drilling and mining.

Total releases are computed by the code CCDFGF (see Section 3.12). Total releases comprise transport releases and direct releases. Transport releases generally involve movement of radionuclides up an abandoned borehole into the Culebra, then through the Culebra to the LWB. Transport of radionuclides to the Culebra is computed using the codes NUTS and PANEL (see Section 3.4) using the brine flows computed by BRAGFLO (see Section 3.3). Radionuclide transport through the Culebra is computed by the code SECOTP2D (see Section 3.11) using flow fields calculated by MODFLOW 2000 (see Section 3.10).

Direct releases occur at the time of a drilling intrusion and include releases of solids (cuttings, cavings, and spallings) computed using the code CUTTINGS_S (see Sections 3.6 and 3.7) and direct releases of brine computed using BRAGFLO (see Section 3.9). Pressure and brine saturation within the waste areas are used as initial conditions to the models for direct releases. Results from the undisturbed repository (see Section 4) are used as the initial conditions for the first intrusion. To calculate initial conditions for subsequent intrusions, and to compute the source of radionuclides for transport in the Culebra, a set of drilling scenarios are used to calculate conditions within the repository after an intrusion, using BRAGFLO (see Section 3.3).

This section first summarizes the scenarios used to represent drilling intrusions and the resulting repository conditions calculated by BRAGFLO. Next, transport releases are presented, followed by cuttings, cavings, spallings, and DBRs.

5.1 DRILLING SCENARIOS

As shown in Table 5-1, the PA considers two types of drilling intrusions, E1 and E2. The E1 intrusion scenario represents the possibility that a borehole creates a pathway between the repository and a pressurized brine reservoir located within the underlying Castile formation. The E2 intrusion scenario represents a borehole that does not connect the repository with an underlying brine reservoir, but does intrude into the repository. Repository conditions are calculated for the E1 intrusion scenario at 350 and 1,000 years, and are referred to as the BRAGFLO S2 and S3 scenarios, respectively. The BRAGFLO scenarios S4 and S5 represent E2 intrusions that occur at 350 and 1,000 years, respectively. An additional BRAGFLO scenario, S6, simulates the effects of an E2 intrusion at 1,000 years followed by an E1 intrusion 1,000 years later into the same panel.

Table 5-1. WIPP PA modeling scenarios.

Scenario	Description
S1	Undisturbed repository
S2	E1 intrusion at 350 years
S3	E1 intrusion at 1,000 years
S4	E2 intrusion at 350 years
S5	E2 intrusion at 1,000 years
S6	E2 intrusion at 1,000 years; E1 intrusion at 2,000 years

E1: Borehole penetrates through the repository and into a hypothetical pressurized brine reservoir in the Castile formation.

E2: Borehole penetrates the repository, but does not encounter brine reservoir.

5.2 MINING SCENARIOS

Long-term releases within the Culebra could be influenced by future mining activities that remove all the known potash reserves within the LWB and cause the transmissivity within the overlying Culebra to change. The occurrence of the full mining of known potash reserves within the LWB in the absence of active and passive controls is modeled as a Poisson process, with a rate of 10^{-4} yr^{-1} . For any particular future, this rate is used to determine a time at which full mining has occurred. Flow fields are calculated for the Culebra for two conditions: partial mining, which assumes that all potash has been mined from reserves outside the LWB; and full mining, which assumes all reserves have been mined both inside and outside the LWB. Radionuclide transport through the Culebra uses the partial mining flow fields prior to the time at which full mining has occurred and the full mining flow fields after that time.

5.3 SALADO FLOW

This section summarizes the results of the Salado flow calculations for the disturbed scenarios. Nemer (2010) provide a detailed presentation on the BRAGFLO model, calculation results, and further sensitivity analyses.

5.3.1 Pressure in the Repository

Figure 5-1 and Figure 5-2 show pressure in the waste panel for the 100 vectors of replicate R1 for BRAGFLO scenarios S2 and S4, respectively. The pressure exhibits patterns that vary depending on the type of intrusion.

Scenario S2 represents an E1 intrusion at 350 years. At the time of the intrusion, brine flow from the Castile brine reservoir leads to an increase in pressure (Figure 5-1). However, pressure drops sharply 200 years after the intrusion when the borehole plugs above the repository are assumed to fail and the permeability of the borehole generally increases. In vectors with low borehole permeability, pressure does not change noticeably as a result of the borehole plug failure (Nemer 2010).

Scenario S4 represents an E2 intrusion at 350 years. The borehole plugs effectively prevent any change in repository pressure from the time of the intrusion until the borehole plugs fail 200 years after installation (Figure 5-2). As in the scenarios for E1 intrusions, pressure generally drops sharply when the plugs fail, except for vectors with low borehole permeability after plug

failure. The pressure is generally lower in the E2 intrusion scenarios compared with the undisturbed and E1 intrusion scenarios (Nemer 2010).

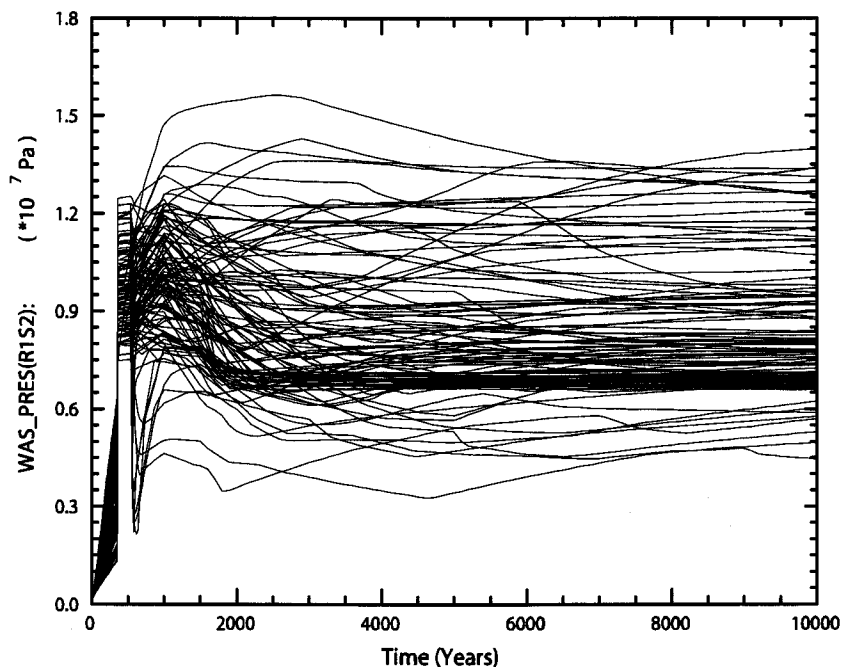


Figure 5-1. Pressure in the Waste Panel region, replicate R1, scenario S2, PABC-2009.

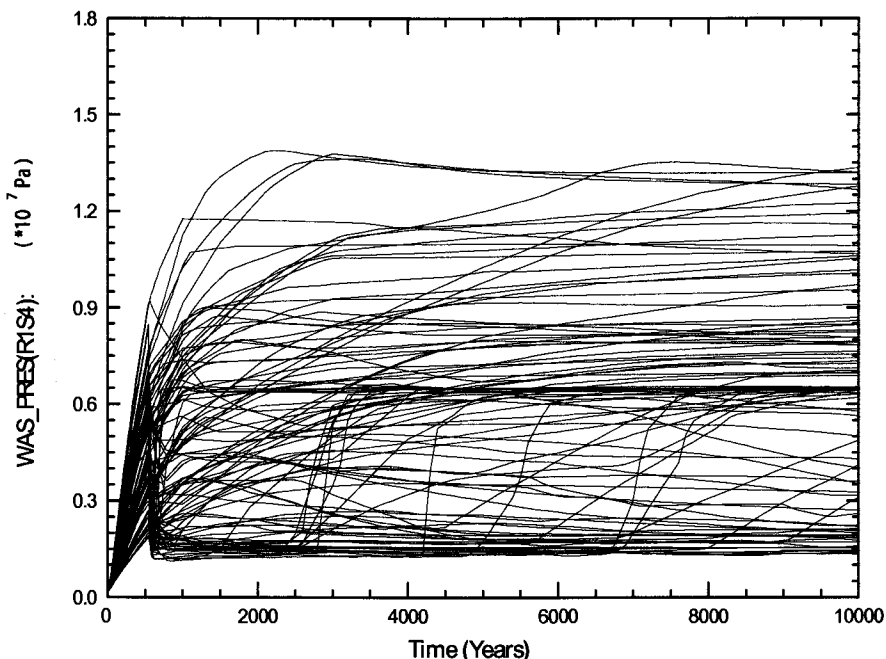


Figure 5-2. Pressure in the Waste Panel region, replicate R1, scenario S4, PABC-2009.

Analysis of the pressure in the waste panel and the uncertain parameters identifies a number of parameters that contribute to the uncertainty in pressure for the disturbed scenarios. The relative importance of these parameters varies over the 10,000-year modeling period. For both scenarios,

the borehole permeability has the largest negative correlation with pressure after the intrusion, as this is the primary means by which pressure may escape the repository in the disturbed scenarios (Nemer 2010).

For scenario S2, the initial Castile brine pocket pressure has the largest positive correlation after the intrusion, while for scenario S4, the largest positive correlation for the majority of the time after the intrusion, results from the halite porosity. The negative correlation of the borehole permeability is larger than the positive correlation of the initial Castile brine pocket pressure and halite porosity for either scenario. The larger initial Castile brine pocket pressure causes more brine at a higher pressure to flow into the repository, while increasing the halite porosity increases the volume of brine available in the material overlying the waste, which, as the brine flows into the waste panel, then increases the amount of brine in the repository. Microbial gas generation rates are a function of the brine in the repository and increase as more brine is available. Increasing the amount of gas generated results in increased repository pressures (Nemer 2010).

The pressure trends in the disturbed scenarios for the PABC-2009 are similar to the results obtained for the CRA-2009 PA. The average and maximum pressures are comparable between the two analyses as well (Nemer 2010, Table 6-16). As the intrusion creates a pathway for brine and gas to flow into and away from the repository, the effects of the changes made for the PABC-2009 are minimized (Nemer 2010). This will translate to a negligible change in spillings and DBR volumes for the second and subsequent intrusions.

5.3.2 Brine Saturation in the Waste

Brine saturation tends to increase after a drilling intrusion. Figure 5-3 and Figure 5-4 show brine saturation in the waste panel for replicate R1 for BRAGFLO scenarios S2 and S4, respectively. Saturation typically increases after an intrusion.

Scenario S2 represents an E1 intrusion at 350 years. At the time of the intrusion, brine flow from the Castile brine reservoir leads to an increase in saturation (Figure 5-3). However, saturation can drop sharply 200 years after the intrusion when the borehole plugs above the repository are assumed to fail and the permeability of the borehole generally increases. In vectors with low borehole permeability, saturation does not change noticeably as a result of the borehole plug failure. Twelve hundred years after the drilling intrusion, the permeability of the borehole connecting the repository to the Castile is assumed to be reduced by an order of magnitude because of creep closure. This material change reduces saturation in some vectors, but does not appear to have a significant effect on the saturation in most vectors (Nemer 2010).

Scenario S4 represents an E2 intrusion at 350 years. The borehole plugs effectively prevent any change in repository saturation from the time of the intrusion until the borehole plugs fail (Figure 5-4). Unlike the E1 intrusion scenarios, saturation generally increases sharply when the plugs fail, except for vectors with low borehole permeability after plug failure. The saturation is generally lower in the E2 intrusion scenarios compared with the E1 intrusion scenarios (Nemer 2010).

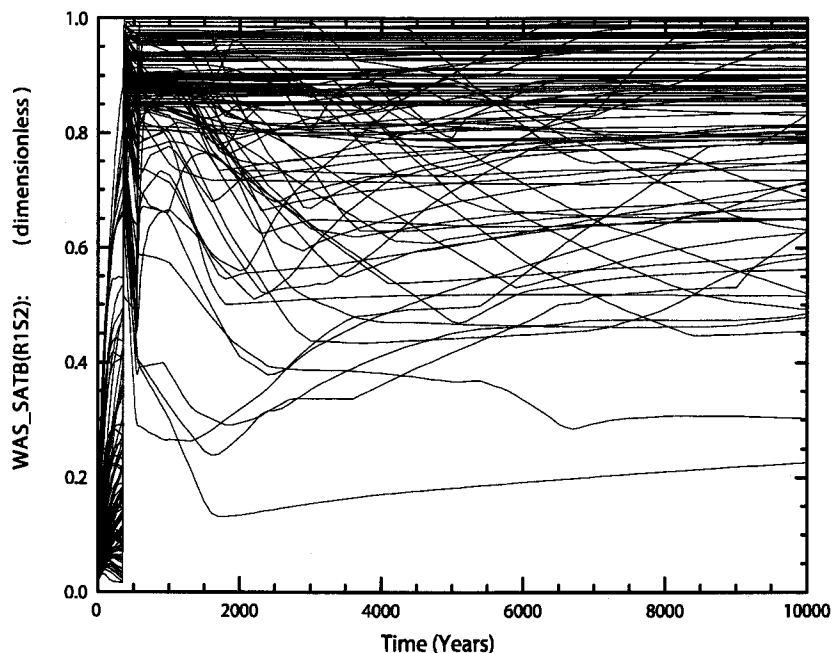


Figure 5-3. Brine saturation in the Waste Panel region, replicate R1, scenario S2, PABC-2009.

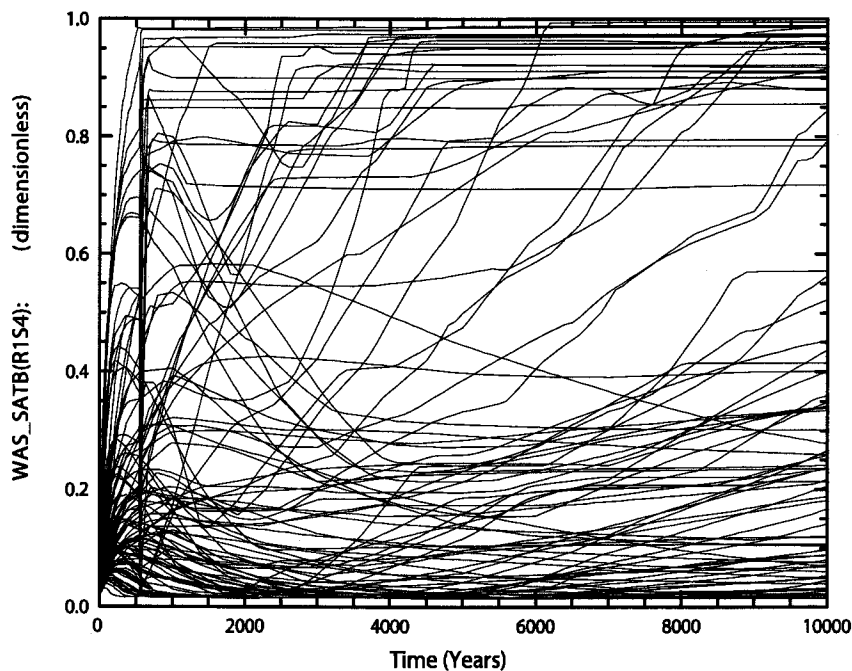


Figure 5-4. Brine saturation in the Waste Panel region, replicate R1, scenario S4, PABC-2009.

Analysis of the brine saturation in the waste panel and the uncertain parameters identifies a number of parameters that contribute to the uncertainty in brine saturation for the disturbed scenarios. The relative importance of these parameters varies over the 10,000-year modeling period.

For scenario S2, the DRZ permeability and the borehole permeability have positive correlations. Increases in DRZ and borehole permeability accelerate brine flow into the waste. The corrosion rate for steel and the waste wicking parameter are negatively correlated with the saturation, as these control the brine consuming reactions. The halite porosity has a high positive correlation before the intrusion, which then decreases.

For scenario S4, the largest positive correlation results from borehole permeability, with the DRZ permeability, anhydrite permeability and the halite porosity also showing high positive correlations. Increases in DRZ, borehole and anhydrite permeability accelerate brine flow into the waste, while increases in halite porosity increase the volume of brine available in the material overlying the waste, all of which control the amount of brine flow into and out of the repository. The corrosion rate for steel is negatively correlated with the saturation as this is a brine consuming reaction.

The brine saturation trends in the disturbed scenarios for the PABC-2009 are similar to the results obtained for the CRA-2009 PA. The average brine saturations are comparable between the two analyses as well (Nemer 2010, Table 6-15). As the intrusion creates a pathway for brine and gas to flow into and away from the repository, the effects of the change made for PABC-2009 are minimized (Nemer 2010). This will translate to a negligible change in DBR volumes for the second and subsequent intrusions.

5.3.3 Brine Flow Out of the Repository

This section describes the flow of brine up a borehole to the Culebra. Brine flow to the Culebra is important in calculating long-term releases to the Culebra. Direct brine flow up the borehole to the surface at the time of drilling is modeled separately in the DBR calculations, presented in Section 5.5.4.

Figure 5-5 shows cumulative brine volume flowing out of the repository (BRNREPOC) for scenario S2. Scenario S2 represents an E1 intrusion at 350 years. At the time of the intrusion, brine from the Castile brine reservoir fills the repository. At 200 years after the intrusion when the borehole plugs above the repository are assumed to fail and the permeability of the borehole generally increases, most of the brine leaving the repository flows up the borehole to the Culebra. In vectors with low borehole permeability, the brine flow rate out of the repository does not change noticeably as a result of the borehole plug failure. Twelve hundred years after the drilling intrusion, the permeability of the borehole between the repository and the Castile is reduced by an order of magnitude because of creep closure, reducing the brine flow rate into the repository and causing a corresponding decrease in brine out of the repository. This material change reduces brine flow rate out of the repository in some vectors, but does not appear to have a significant effect on the brine flow rate out of the repository in most vectors (Nemer 2010).

Figure 5-6 shows the volumes of brine that cross the LWB through the MBs for scenario S2. The largest volume that crosses the LWB is $\sim 1,080 \text{ m}^3$, which is lower than the undisturbed scenario results (see Section 4.1.3). As the intrusion creates a pathway to the Culebra, brine flow to the LWB is reduced. Brine crossing the LWB or moving up the shaft does not necessarily indicate releases from the repository, since the brine may not have been in contact with the waste; the brine may have been present in the MBs at the start of the regulatory period. Section

5.4 presents the results of the radionuclide transport calculations that determine the amount of radionuclides that may be released by transport in brine for the disturbed scenarios.

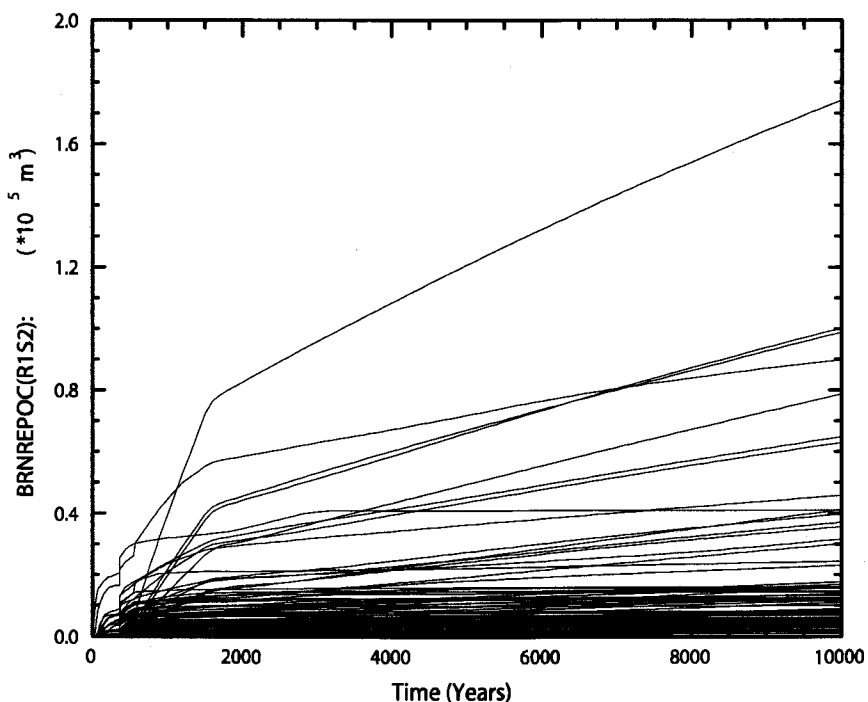


Figure 5-5. Brine volume flowing away from the repository, replicate R1, scenario S2, PABC-2009.

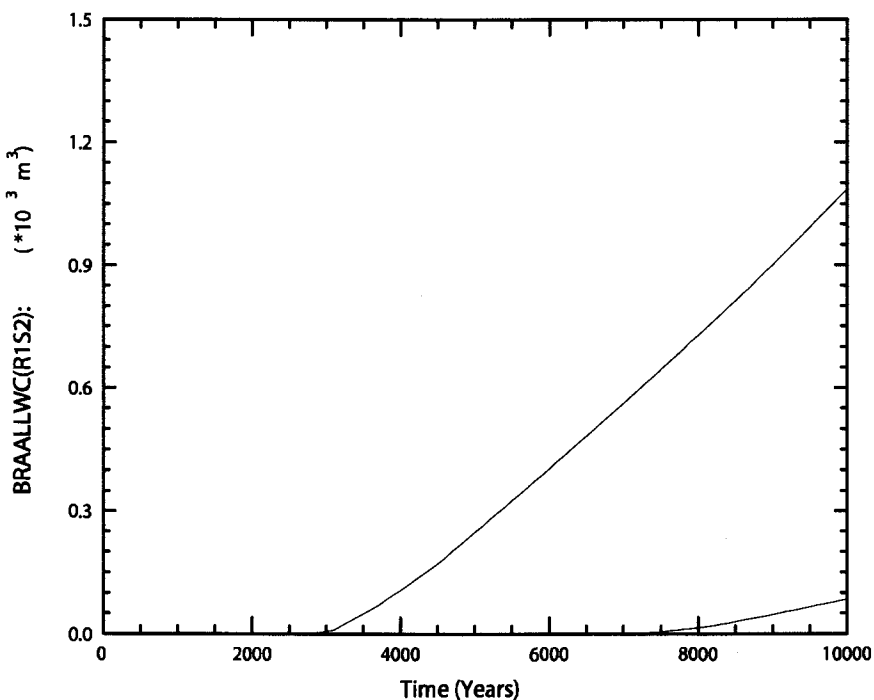


Figure 5-6. Brine volume flowing via all MBs across the LWB, replicate R1, scenario S2, PABC-2009.

Figure 5-7 shows cumulative brine volume flowing out of the repository (BRNREPOC) for the BRAGFLO scenarios S4. Scenario S4 represents an E2 intrusion at 350 years. The results for the S4 scenario are very similar to the results for the undisturbed scenario, S1 (see Section 4.1.3).

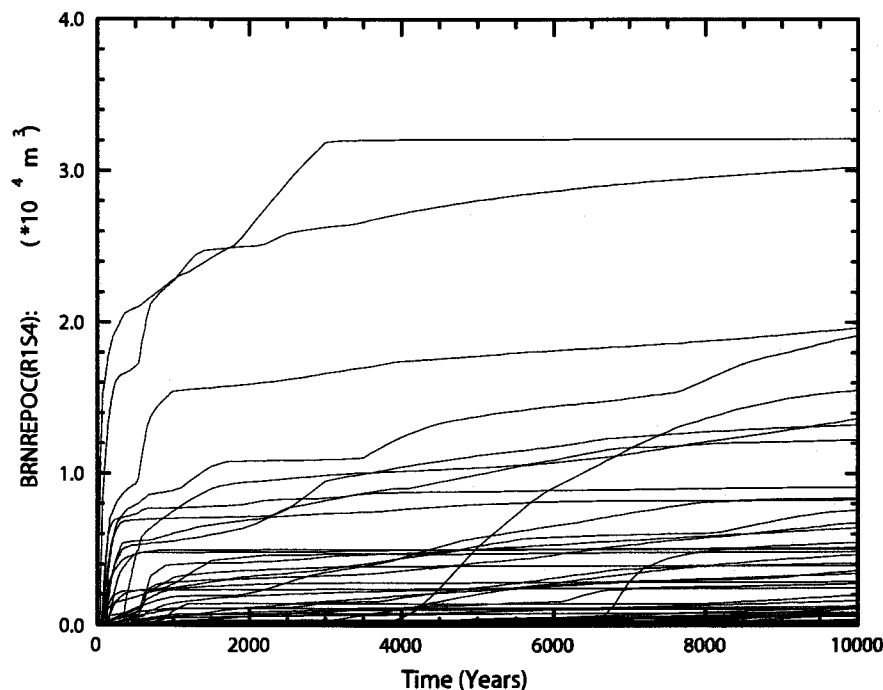


Figure 5-7. Brine volume flowing away from the repository, replicate R1, scenario S4, PABC-2009.

Figure 5-8 shows the volumes of brine that cross the LWB through the MBs for the BRAGFLO scenario S4. The largest volume that crosses the LWB is $\sim 1,010 \text{ m}^3$, which is smaller than the undisturbed scenario results (see Section 4.1.3). As the intrusion creates a pathway to the Culebra, the brine flow rate to the LWB is reduced. Brine crossing the LWB or moving up the shaft does not necessarily indicate releases from the repository, since the brine may not have been in contact with the waste; the brine may have been present in the MBs at the start of the regulatory period. Section 5.4 presents the results of the radionuclide transport calculations that determine the amount of radionuclides that may be released by transport in brine for the disturbed scenarios.

Regression between total cumulative brine volume flowing out of the waste-filled regions (BRNREPOC) and the uncertain parameters for the BRAGFLO scenarios S2 and S4, show that the permeability of the DRZ, the borehole permeability and the porosity of undisturbed halite have positive correlations. Increases in the DRZ and borehole permeability allow more brine to flow out of the repository. The increase in the halite porosity is correlated with the increase in pressure (see Section 5.3.1), and an increase in pressure increases the brine flow rate out of the repository. A negative correlation with the waste residual brine saturation is shown for both the S2 and S4 scenarios, which determines the immobile portion of the waste brine saturation, which then limits the amount of brine that can flow out of the waste-filled regions.

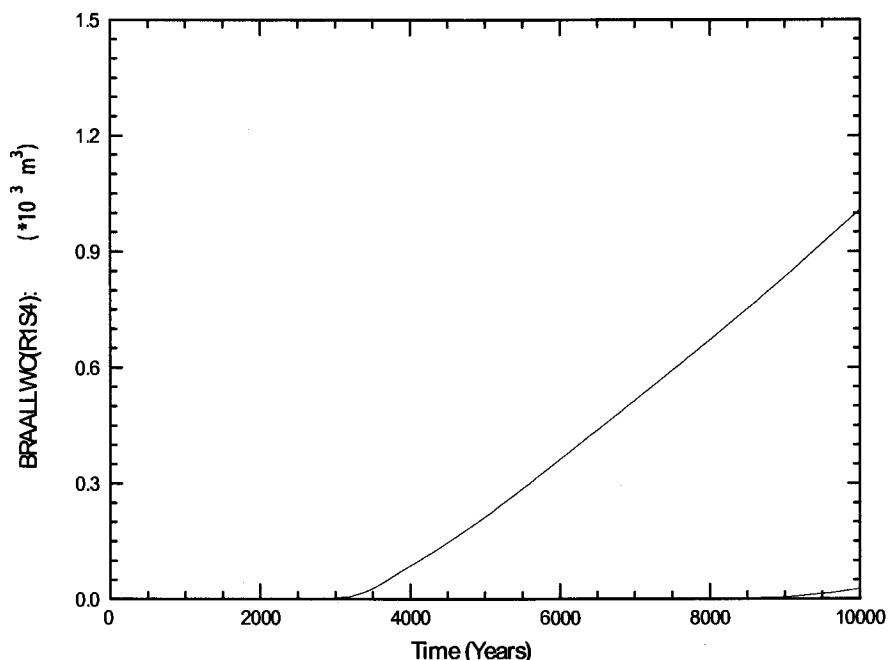


Figure 5-8. Brine volume flowing via all MBs across the LWB, replicate R1, scenario S4, PABC-2009.

The permeability of the concrete panel seal is negatively correlated for the S2 scenario and positively correlated for the S4 scenario. The increased permeability of the concrete panel seal allows more brine to flow from the intruded panel to the remainder of the repository (flow into another panel is not considered out of the repository), reducing the higher pressure conditions in the intruded panel in the S2 scenario and therefore the flow rate out of the repository through the borehole, while for the S4 scenario, the increased permeability allows the brine from the remainder of the repository to flow into the depressurized intruded panel, increase the pressure and flow out of the repository up the borehole.

The total cumulative brine volume flowing away from the repository in the disturbed scenarios for the PABC-2009 is similar to the results obtained for the CRA-2009 PA (Nemer 2010, Table 6-17). The average and maximum cumulative brine volumes to the LWB through the MBs are lower for the PABC-2009 compared with the CRA-2009 PA (Nemer 2010, Table 6-18). As the intrusion creates a pathway for brine and gas to flow into and away from the repository, the effects of the changes made for the PABC-2009 are minimized (Nemer 2010).

5.4 RADIONUCLIDE TRANSPORT

In the disturbed scenarios, radionuclide transport through the marker beds in the Salado is calculated by the code NUTS (see Section 3.4). Radionuclide transport from the through the borehole to the Culebra is calculated by NUTS and PANEL (see Section 3.4). Radionuclide transport within the Culebra is calculated by SECOTP2D (see Section 3.11). For all radionuclide transport calculations, mobilized concentrations of radionuclides in Salado and Castile brines are computed by the code PANEL (see Section 3.8).

This section summarizes the radionuclide transport results for the disturbed scenarios. Nemer (2010) describe the brine and gas flow in the Salado. Detailed analysis of the radionuclide transport in the Salado is presented in Ismail and Garner (2010). Garner (2010) provides an analysis of the mobilized concentrations of radionuclides in Salado and Castile brines; Kuhlman (2010) presents an analysis of the flow and radionuclide transport within the Culebra.

5.4.1 Radionuclide Source Term

The code PANEL calculates the time-varying concentration of radionuclides mobilized in brine, either as dissolved isotopes or as isotopes sorbed to mobile colloids. Two different brines are considered: the interstitial brine present in the Salado Formation called GWB, which is magnesium rich; and the brine in the Castile Formation called ERDA-6, which is sodium rich. Radionuclide solubility in the two brines can be considerably different. Before an E1 intrusion, performance assessment assumes that the brine in the repository is GWB. After an E1 intrusion, brine in the repository is assumed to be ERDA-6 brine.

Figure 5-9 and Figure 5-10 show the concentration of radioactivity mobilized in Salado and Castile brines, respectively, as a function of time for all vectors in replicate R1 for the PABC-2009. Concentrations are expressed as EPA units/m³ to combine the radioactivity of different isotopes. The differences between the results in the Salado brine compared with the Castile brine are minimal.

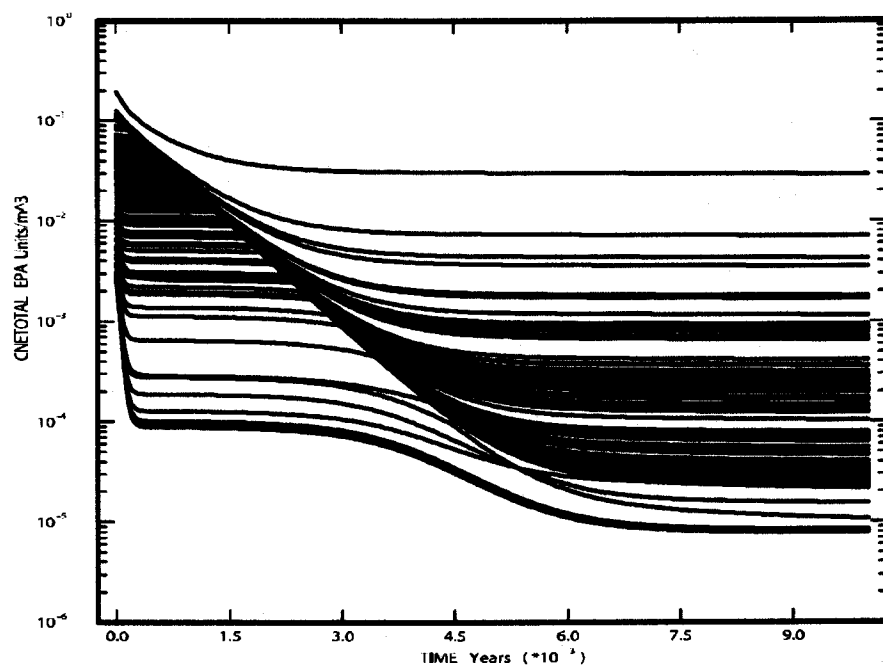


Figure 5-9. Total mobilized concentrations in Salado brine, replicate R1, PABC-2009.

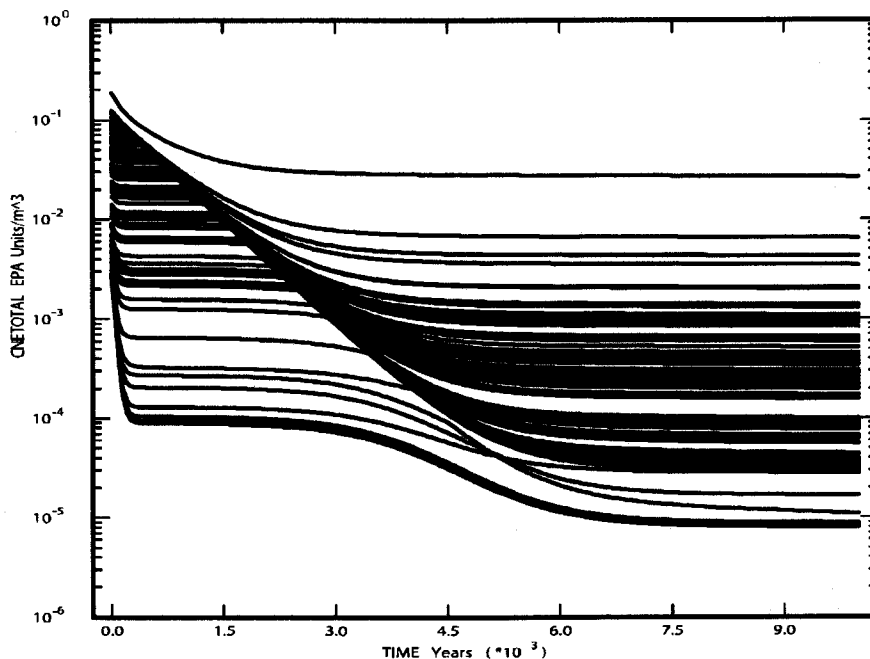


Figure 5-10. Total mobilized concentrations in Castile brine, replicate R1, PABC-2009.

Short-lived radionuclides, such as ^{238}Pu , decay rapidly in the first few years. At early times, the mobilized concentration is dominated by Am; the concentration of Am is limited by its solubility until all the inventory of Am is in solution. After all Am is in solution, the total radionuclide concentration generally decreases as the Am decays, until the mobilized concentration becomes dominated by Pu (Garner 2010). The horizontal lines in the figures indicate periods of time when the total radionuclide concentration is limited by the solubility of Am (before about 3,000 years) or Pu (after about 6,000 years). Thus, the uncertainty in total radionuclide concentration is determined by the uncertainty factors used in the calculation of solubilities for Am and Pu (Garner 2010).

Compared with the CRA-2009 PA, the baseline solubility limit for the III actinides increased due to the updated inventory (see Section 2.2). Since the dominant radionuclides, Am and Pu, are modeled as III actinides for 100% and 50% of the vectors, respectively, the increase in the baseline solubility limit increased the total radionuclide concentration. An increase in the total radionuclide concentration is expected to increase radionuclide transport through the borehole, as well as DBRs.

5.4.2 Through the Shaft

For the disturbed repository, no vectors showed radionuclide transport through the shafts to the Culebra. Consequently, no radionuclides could be transported through the Culebra to the accessible environment under disturbed conditions (Ismail and Garner 2010).

5.4.3 Through the Marker Beds

In the disturbed scenarios, of the 300 realizations, only vector 53 in replicate R1 resulted in transport of radionuclides through the MBs and across the LWB, with a maximum total

integrated activity of 6.3×10^{-11} EPA units (Ismail and Garner 2010). This is less than the CRA-2009 PA results for maximum integrated activity which had 3.6×10^{-10} EPA units at the boundary (Ismail and Garner 2008). The releases through the MBs and across the LWB are insignificant when compared to releases from drilling intrusions.

5.4.4 Through the Borehole

Radionuclide transport to the Culebra via a single intrusion borehole (disturbed scenarios S2, S3, S4, and S5) is modeled with the code NUTS. Transport to the Culebra in the multiple intrusion scenario (S6), is modeled with the code PANEL. Detailed discussion of the radionuclide transport to the Culebra calculations can be found in Ismail and Garner (2010).

Figure 5-11 through Figure 5-15 show cumulative radioactivity transported up the borehole to the Culebra in the intrusion scenarios. Transport to the Culebra is larger and occurs for more vectors in the S2, S3 and S6 scenarios (with E1 intrusions) than in the S4 or S5 scenarios (E2 intrusions only). For most vectors that show significant transport, most of the transport occurs over a relatively short period of time, immediately after the borehole plugs fail. For the S6 scenario, only two vectors show radionuclide transport after the E2 intrusion at 1,000 years; most radionuclide transport occurs immediately following the E1 intrusion at 2,000 years.

When compared with the results of the CRA-2009 PA, the PABC-2009 showed an increase in the maximum and average releases (Ismail and Garner 2010). The primary change for the PABC-2009 that affected the transport to the Culebra calculations is the update to the inventory (see Section 2.1) and the actinide solubility limits (see Section 2.2). An increase in releases to the Culebra is expected (Ismail and Garner 2010).

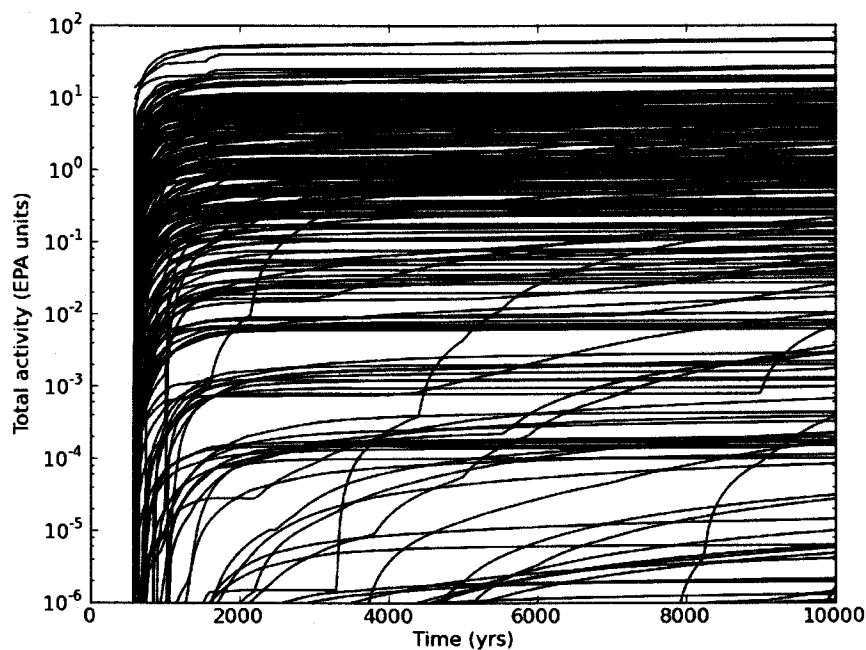


Figure 5-11. Cumulative normalized release to the Culebra, scenario S2, PABC-2009.

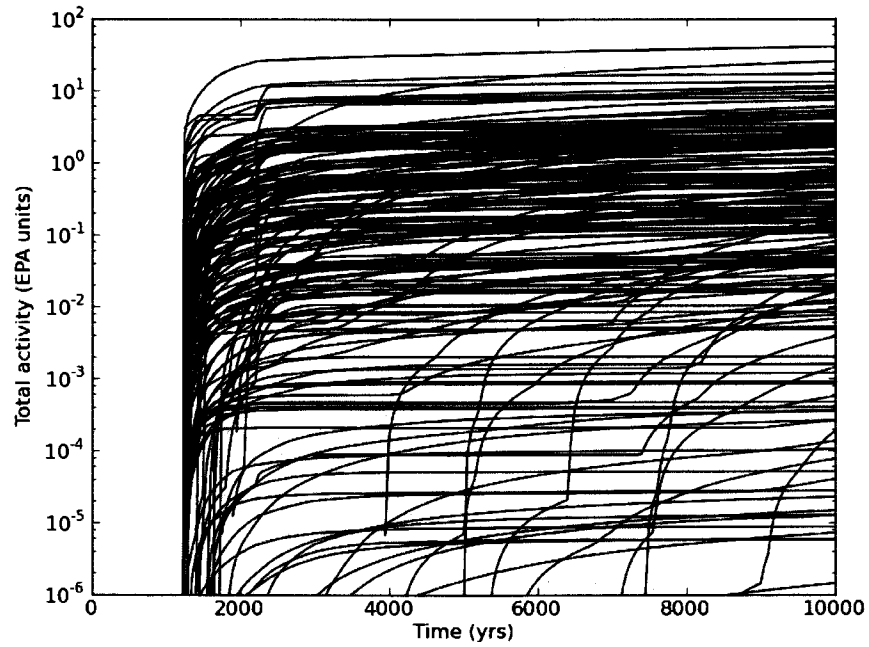


Figure 5-12. Cumulative normalized release to the Culebra, scenario S3, PABC-2009.

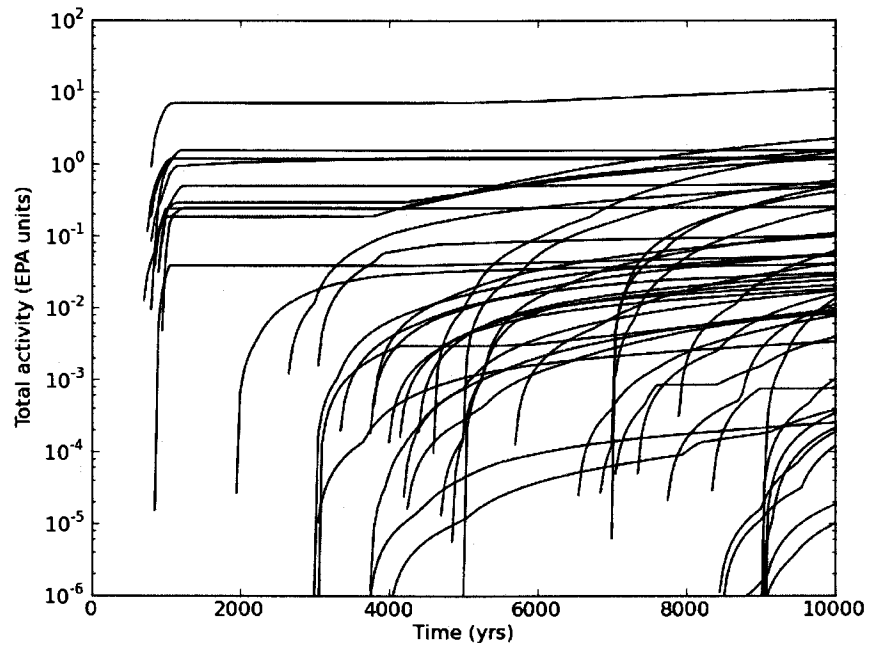


Figure 5-13. Cumulative normalized release to the Culebra, scenario S4, PABC-2009.

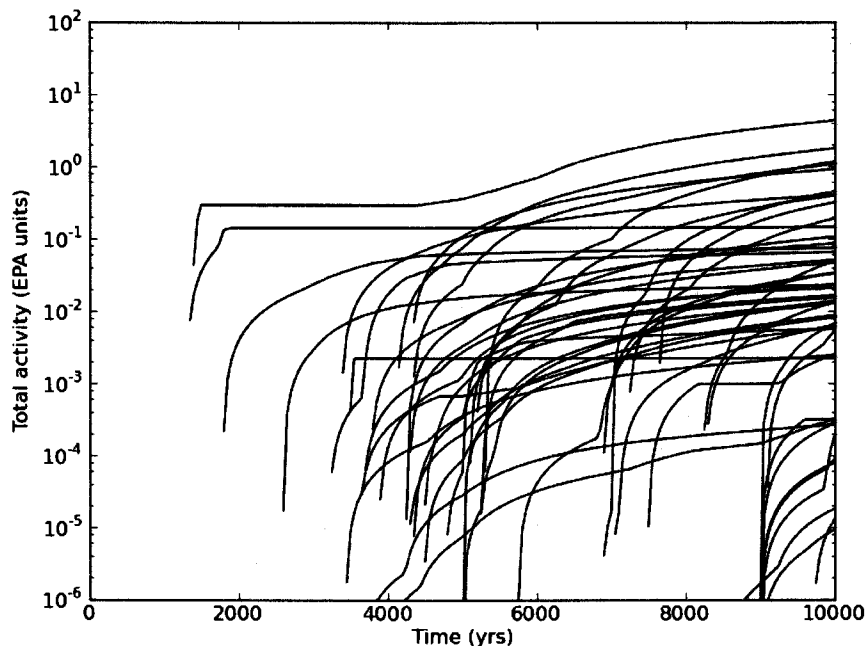


Figure 5-14. Cumulative normalized release to the Culebra, scenario S5, PABC-2009.

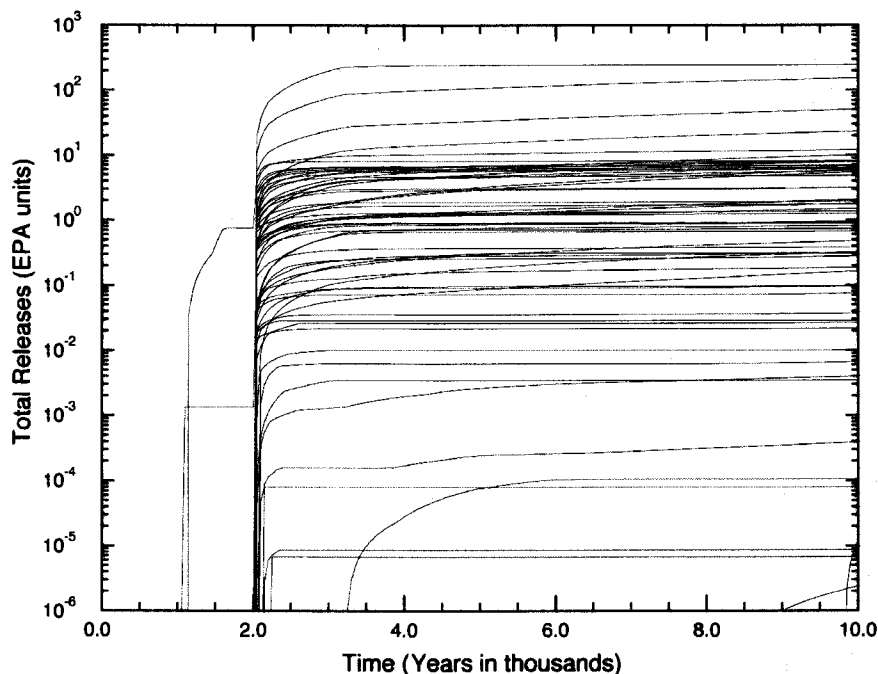


Figure 5-15. Cumulative normalized release to the Culebra, scenario S6, PABC-2009.

5.4.5 Through the Culebra

Radionuclide transport through the Culebra for a given set of uncertain parameters is calculated with the code SECOTP2D (see Section 3.11). Note that the total release of radionuclides across the LWB at the Culebra for given futures is calculated with the code CCDFGF by convolving the SECOTP2D results with the radionuclide transport to the Culebra calculated by NUTS and

PANEL. This section discusses the SECOTP2D results; total releases from the Culebra are presented in Section 6.4.

Culebra radionuclide transport calculations were performed for three replicates of 100 vectors each for both partial-mining and full-mining scenarios (600 total simulations). Each of the 600 radionuclide transport simulations used a unique flow field computed separately with the code MODFLOW 2000 (see Section 3.10 and Kuhlman 2010). The partial mining scenario assumes the extraction of all potash reserves outside the LWB, while full mining assumes that all potash reserves both inside and outside the LWB are exploited.

In each radionuclide transport simulation, 1 kg of each of four radionuclides (^{241}Am , ^{234}U , ^{230}Th , and ^{239}Pu) are released in the Culebra above the center of the waste panel area. Radionuclide transport of the ^{230}Th daughter product of ^{234}U decay is calculated and tracked as a separate species. In the following discussion, ^{230}Th will refer to the ^{234}U daughter product and ^{230}ThA will refer to that released at the waste panel area.

For the three replicates in the PABC-2009, the number of vectors with cumulative releases greater than 10^{-9} kg is shown in Table 5-2, for each radionuclide, under partial and full mining conditions. All SECOTP2D results, regardless of magnitude, are included in the calculation of releases from the Culebra. Under partial and full mining conditions, ^{234}U has the highest number of vectors that surpassed the 10^{-9} kg criterion, while ^{241}Am has the least number of vectors. A considerable increase is observed in the full mining scenario compared with the partial mining scenario, due to the increased proximity of the potash reserves within the LWB to the repository which are extracted in the full mining scenario (Kuhlman 2010).

Table 5-2. PABC-2009 Culebra transport statistics.

# of vectors	Partial Mining			Full Mining		
	R1	R2	R3	R1	R2	R3
^{241}Am	0	0	0	8	10	3
^{239}Pu	3	1	1	20	27	22
^{234}U	11	14	12	48	50	47
^{230}Th	5	10	6	36	38	42
^{230}ThA	2	3	0	21	31	29

Compared with the results from the CRA-2004 PABC, there is a large increase in the transport of radionuclide through the Culebra to the LWB. This increase can be attributed to three factors (Kuhlman 2010):

1. Changes in the definition of minable potash
2. Changes in the lower limit of the K_d ranges (see Section 2.5), and
3. Updates to the Culebra transmissivity fields (see Section 2.3).

With the large increase in the radionuclide transport through the Culebra, an increase of releases from the Culebra is expected.

5.5 DIRECT RELEASES

Direct releases occur at the time of a drilling intrusion, and include cuttings and cavings; spillings; and DBRs. This section presents an analysis of the volume released by each mechanism, along with the source term used for the calculation of direct solid releases. The source term used for the calculation of DBRs is discussed in Section 5.4.1. Garner (2010) provides an analysis of the mobilized concentrations of radionuclides in Salado and Castile brines. Fox and Clayton (2010) provide a summary and analysis of the solid release source term. Ismail (2010) provides additional information about the cuttings, cavings and spillings releases calculated for the PABC-2009. Clayton (2010a) provides a detailed analysis of direct brine releases in the PABC-2009.

5.5.1 Solid Source Term

The code EPAUNI calculates the time varying activity of the waste, accounting for radioactive decay, which is used in calculating direct solid releases during a drilling intrusion. The radionuclide content of the waste encountered depends on the waste stream encountered. The waste is assumed to be emplaced randomly in the repository and the probability of encountering any given waste stream is directly proportional to the volume of that waste stream. The probability of encountering each waste stream, as well as its time dependent radionuclide content is calculated for each waste stream. Ten radionuclides are modeled for the solid releases source term: ^{241}Am , ^{244}Cm , ^{137}Cs , ^{238}Pu , ^{239}Pu , ^{240}Pu , ^{241}Pu , ^{90}Sr , ^{233}U , and ^{234}U , as these account for 99.98% of the EPA units at the time of repository closure (Fox et al. 2009).

For the entire inventory, the total EPA Units as a function of time, along with four individual radionuclides that appreciably contribute to the total for the PABC-2009 are shown in Figure 5-16. The initial normalized activity of the inventory is dominated by ^{241}Am , ^{238}Pu , ^{239}Pu and ^{240}Pu . The ^{241}Am and ^{238}Pu decay rapidly and so the total normalized activity of the inventory is dominated at later times (>2,000 years) by mainly ^{239}Pu with a small contribution from the ^{240}Pu (Fox and Clayton 2010).

Comparing the normalized activities for the PABC-2009 and the CRA-2009 PA inventories, the total EPA units for both inventories start at similar levels. The PABC-2009 results are lower after ~350 years and then remain lower throughout the 10,000-year regulatory period (Fox and Clayton 2010). This is expected to decrease the direct solid releases for the PABC-2009, as the majority of the intrusions into the repository occur after 350 years from closure.

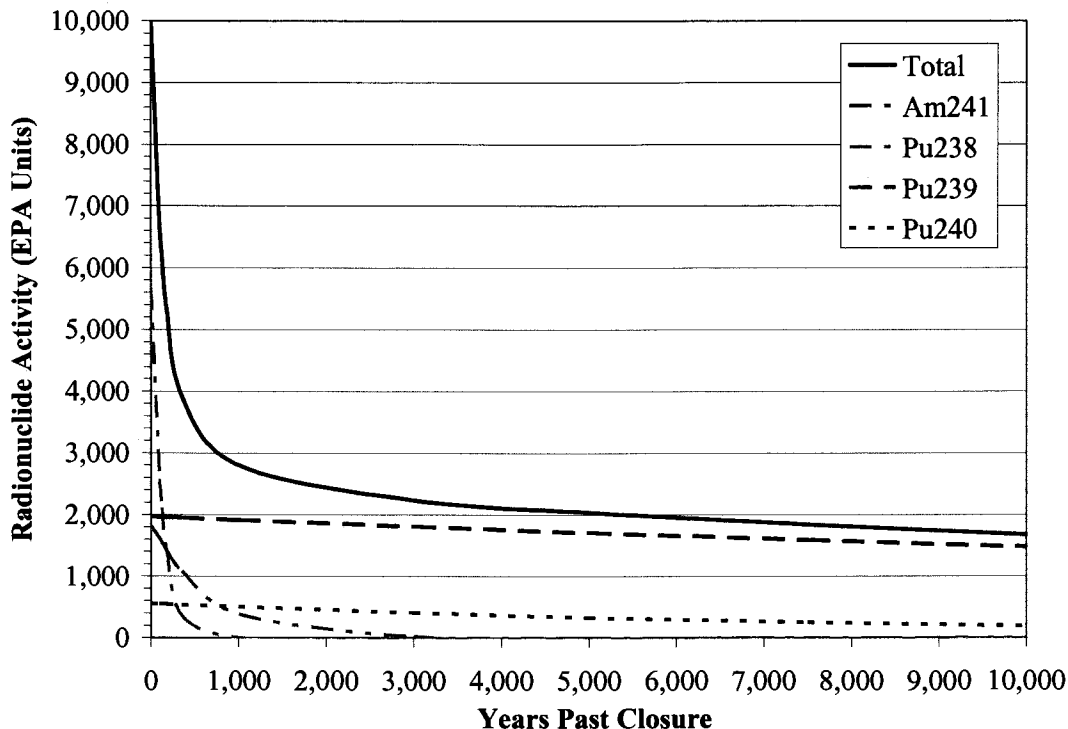


Figure 5-16. Total and individual normalized radionuclide activity from closure to 10,000 years, PABC-2009.

5.5.2 Cuttings and Cavings

Cuttings and cavings are the solid waste material removed from the repository and carried to the surface by the drilling fluid during the process of drilling a borehole. Cuttings are the materials removed directly by the drill bit, and cavings are the material eroded from the walls of the borehole by shear stresses from the circulating drill fluid. The volume of cuttings and cavings material removed from a single drilling intrusion into the repository is assumed to be in the shape of a cylinder. The code CUTTINGS_S calculates the area of the base of this cylinder, and cuttings and cavings results in this section are reported in terms of these areas. The volumes of cuttings and cavings removed can be calculated by multiplying these areas with the initial repository height, 3.96 m (BLOWOUT:HREPO).

Cuttings and cavings areas calculated for the PABC-2009 range between 0.076 m² and 0.86 m², with a mean area of 0.25 m² (Table 5-3). None of the changes implemented in the PABC-2009 affect the cuttings and cavings calculations, and so the results are identical to the CRA-2009 PA results (Ismail 2010).

Table 5-3. PABC-2009 cuttings and cavings area statistics.

Replicate	Min (m ²)	Max (m ²)	Mean (m ²)	Vectors w/o Cavings
R1	0.076	0.82	0.25	9
R2	0.076	0.86	0.25	10
R3	0.076	0.83	0.25	11

Two uncertain sampled parameters affect the cavings calculations. The uncertainty in cavings areas arises primarily from the uncertainty in the shear strength of the waste (Ismail 2010). Lower shear strengths tend to result in larger cavings (Figure 5-17). The uncertainty in the drill string angular velocity has a smaller impact on the cavings results, but the combination of a low angular velocity and high shear strength can prohibit cavings from occurring. In fact, cavings did not occur in ten percent of all vectors (Table 5-3).

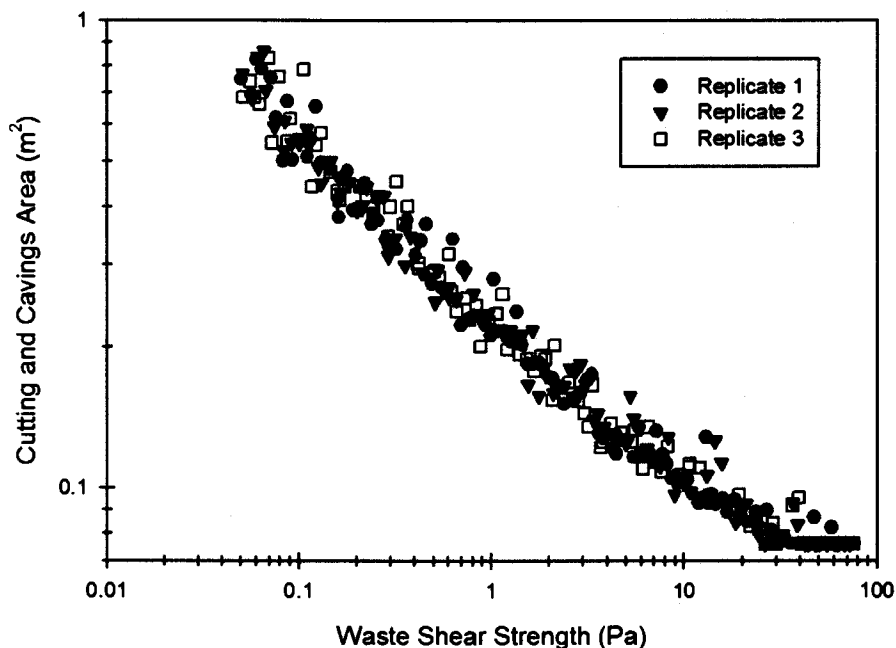


Figure 5-17. Scatter plot of cuttings and cavings areas versus shear strength, PABC-2009.

5.5.3 Spallings

Calculation of the volume of solid waste material released to the surface from a single drilling intrusion into the repository due to spallings is a two-part procedure. The code DRSPALL calculates the spallings volumes from a single drilling intrusion at four values of repository pressure (10, 12, 14, and 14.8 MPa). The second step in calculating spallings volumes from a single intrusion consists of using the code CUTTINGS_S to interpolate the DRSPALL volumes. The spallings volume for a vector is then determined in CUTTINGS_S by linearly interpolating the volume calculated by DRSPALL based on the pressure calculated by BRAGFLO. Results from both of these calculations are documented in this section.

The code DRSPALL was run for each of 100 vectors in three replicates and for four values of repository pressure (10, 12, 14, and 14.8 MPa). No spallings occurred at 10 MPa for any vector. None of the changes implemented in the PABC-2009 and CRA-2009 PA affect the DRSPALL calculations, and so the results from the CRA-2004 PABC were used in the PABC-2009.

The uncertainty in the spallings volumes arises from four variables that are uncertain in the DRSPALL calculations: waste permeability, waste porosity, waste tensile strength, and waste particle diameter after tensile failure. The largest spallings volumes occur when waste permeability is less than $1.0 \times 10^{-13} \text{ m}^2$, but larger permeability values result in a higher frequency

of nonzero spillings volumes. This observation can be explained as follows: the higher permeability values that were sampled result in smaller tensile stresses and less tensile failure, but promote fluidization. Lower permeability leads to greater tensile stresses and tensile failure, but failed material may not be able to fluidize at this low permeability. Smaller particle diameter values tend to result in larger spillings volumes and a higher frequency of nonzero spillings volumes. The uncertainty in the spillings volumes from a single intrusion is largely determined by the uncertainty in these two parameters. Obvious correlations between spillings volumes and the two other parameters could not be established (Vugrin 2005).

Utilizing the volumes calculated by DRSPALL and the repository pressures calculated by BRAGFLO, the spillings volumes for the PABC-2009 can be calculated. Table 5-4 summarizes the statistics for the PABC-2009 spillings volumes. The scenarios shown in Table 5-4 indicate the state of the repository before the intrusion. The results shown for scenario S1 represent the first intrusion into an undisturbed repository, while the results shown for scenarios S2 through S5 represent the second or subsequent intrusion into a disturbed repository.

Table 5-4. PABC-2009 spillings volume statistics.

Scenario	Max volume (m ³)			Average volume (m ³)			Number of nonzero volumes		
	R1	R2	R3	R1	R2	R3	R1	R2	R3
S1	2.24	2.36	4.91	0.03	0.03	0.05	142	168	156
S2	8.29	2.76	6.23	0.04	0.03	0.03	117	122	113
S3	7.97	1.86	2.62	0.04	0.03	0.02	111	122	118
S4	1.67	2.26	1.47	0.01	0.02	0.01	59	57	45
S5	1.67	1.93	1.49	0.02	0.03	0.01	77	84	72
All	8.29	2.76	6.23	0.03	0.03	0.02	506	553	504

Of the 7,800 (26 intrusion time-scenario combinations × three drilling locations × 100 vectors) spillings volumes calculated per replicate, more than 93% of each replicate’s calculations resulted in no spillings. Only about a third of the vectors in each replicate had spillings occur in at least one of the scenarios. Therefore spillings will not contribute to the total releases calculated for the other vectors.

Scenarios S2 and S3 resulted in the largest maximum spillings volume, while scenarios S1, S2 and S3 resulted in the largest average spillings volume. Scenarios S2 and S3 have the highest maximum pressures because in these scenarios, the drill bit intrudes into a pressurized brine pocket (Nemer 2010). These higher pressures lead to larger spillings volumes. Scenarios S4 and S5 resulted in the lowest maximum and average volumes as in general these scenarios have the lowest pressure (see Section 5.3.1). Scenario S1 resulted in the largest number of nonzero spillings volumes per time intrusion. Without an intrusion to create a pathway for brine and gas flow to decrease the pressure, there are more vectors that result in pressures above 10 MPa and hence a nonzero spillings volume.

The frequency of nonzero spillings volumes decreased for the PABC-2009 compared with the CRA-2009 PA (Ismail 2010, Table 7). The PABC-2009 maximum and average spillings volumes decreased versus the CRA-2009 PA results (Ismail 2010, Table 7). As the spillings volumes are calculated from BRAGFLO pressure and a decrease in pressure was observed (see Sections 4.1.1 and 5.3.1), a decrease in the spillings releases is expected.

5.5.4 Direct Brine Releases

DBRs to the surface can occur during or shortly after a drilling intrusion. For each element of the Latin hypercube sample, the code BRAGFLO calculates volumes of brine released for a total of 78 combinations of intrusion time (six for scenario S1, five for scenarios S2-S5), intrusion location (three locations), and initial conditions (five scenarios). Initial conditions for the DBR calculations are obtained from the BRAGFLO Salado flow modeling results from scenarios S1 through S5. Salado flow modeling results from the S1 scenario (Section 4.1) are used as initial conditions for DBR for a first intrusion into the repository which may have a DBR. Salado flow modeling results from the S2 through S5 scenarios (Section 5.3) are used as initial conditions for DBR for second or subsequent drilling intrusions that may have a DBR.

Summary statistics of the calculated DBR volumes for replicate R1 of the PABC-2009 are shown in Table 5-5. As seen in Table 5-5, 996 of the 7,800 DBR calculations (100 vectors \times 78 combinations) resulted in a nonzero DBR volume to the surface, the majority of which resulted from scenarios S2 and S3. The maximum DBR volume is approximately 42 m³, with an average volume of 0.9 m³. DBR volumes are larger and occur more frequently in the S2 and S3 scenarios, because the repository has a much higher saturation after an E1 intrusion (Clayton 2010a).

Table 5-5. PABC-2009 DBR volume statistics.

Scenario	Max volume (m ³)	Average volume (m ³)	Number of nonzero volumes
S1	16	0.1	122
S2	42	2.9	388
S3	41	1.5	310
S4	19	0.1	74
S5	20	0.1	102
All	42	0.9	996

Sensitivity analyses have determined that a DBR volume from a single intrusion is most sensitive to the initial pressure and brine saturation in the intruded panel. The initial pressure and brine saturation in the DBR calculations are transferred from the Salado flow calculations as described above. Thus, the uncertain parameters that are most influential to the uncertainty in pressure and brine saturation in the Salado flow calculations (see Sections 4.1 and 5.3) are also most influential in the uncertainty in DBR volumes.

The combination of relatively high pressure and brine saturation in the intruded panel is required for direct brine release to the surface. Figure 5-18 shows a scatter plot of pressure in the waste panel versus DBR volumes for scenario S2, with symbols indicating the value of the mobile brine saturation (defined as brine saturation minus residual brine saturation in the waste). Above 8 MPa (indicated by the vertical line), a number of vectors have zero releases, but these vectors have mobile brine saturations less than zero and thus no brine is available to be released. When mobile brine saturation approaches 1, relative permeability of the gas becomes small enough that no gas flows into the well, and in these circumstances DBR releases end after three days. Thus, in vectors with high mobile brine saturations, DBR releases increase proportionally with increases in pressure, as evidenced by the linear relationship between DBR volume and pressure

for mobile brine saturation between 0.8 and 1.0. For vectors with mobile saturations between 0.2 and 0.8, both gas and brine can flow in the well, and the rate of gas flow can be high enough that the ending time of DBR releases may be as long as 4.5 days. Although brine may be flowing at slower rates in these vectors than in vectors with high mobile saturations, brine flow may continue longer and thus result in larger DBR volumes.

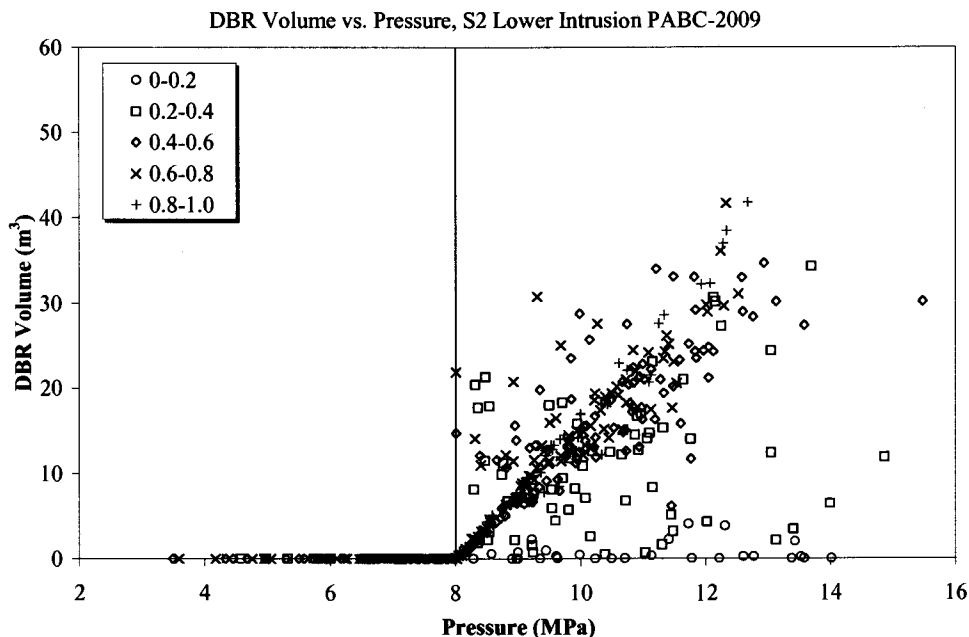


Figure 5-18. Sensitivity of DBR volumes to pressure and mobile brine saturation, replicate R1, scenario S2, Lower panel, PABC-2009. Symbols indicate the range of mobile brine saturation given in the legend.

The frequency of nonzero DBR volumes and the maximum DBR volumes decreased for the PABC-2009 compared with the CRA-2009 PA (Clayton 2010a, Table 6-1). The PABC-2009 average DBR volume is similar compared with the CRA-2009 PA results (Clayton 2010a, Tables 6-2 through 6-5). Since the DBR volumes for the PABC-2009 are similar to the CRA-2009 PA, a minimal impact on DBRs is expected (Clayton 2010a).

6. NORMALIZED RELEASES

This section presents a discussion of each of the four categories of releases that constitute the total release: cuttings and cavings; spallings; DBRs; and subsurface transport releases, followed by the total normalized releases for the PABC-2009. The overall mean CCDF is computed as the arithmetic mean of the mean CCDFs from each replicate. In summary, despite the changes made between the PABC-2009 and the CRA-2009 PA, cuttings, cavings and DBRs remain the most significant pathways for release of radioactive material to the land surface. Release by spallings and subsurface transport in the Salado or Culebra make essentially no contribution to total releases. Finally, the resulting CCDFs of both analyses are within regulatory limits.

6.1 CUTTINGS AND CAVINGS

The overall mean CCDFs for cuttings and cavings releases from the PABC-2009 and the CRA-2009 PA are shown in Figure 6-1. The resulting overall mean CCDFs are very similar in shape, with a decrease in the PABC-2009 compared with the CRA-2009 PA. A minimal difference is observed when comparing the CCDFs for cuttings and cavings volume, therefore, the decrease is due to the updated inventory (Camphouse 2010). As discussed in Section 5.5.1, the solid source term for the PABC-2009 inventory is lower after roughly 350 years and remains lower for the rest of the 10,000-year regulatory period. As a result, the direct solid releases from cuttings and cavings decreased. The rank regression analysis showed that the waste shear strength controls about 98% of the variability in mean cuttings and cavings releases in both the PABC-2009 and CRA-2009 PA (Kirchner 2010b). Cuttings and caving releases are primarily controlled by the volume of cuttings and cavings produced, which in turn is a highly non-linear function of the waste shear strength (Ismail 2010).

6.2 SPALLINGS

Figure 6-2 shows the overall mean spallings release CCDFs from the PABC-2009 and the CRA-2009 PA. The resulting overall mean CCDFs are very similar in shape, with a decrease in the PABC-2009 compared with the CRA-2009 PA. A decrease is observed for the PABC-2009 when comparing the CCDFs for spallings volume (Camphouse 2010), which is due to the lower repository pressure observed in the PABC-2009 calculations (Ismail 2010). The spallings releases also decreased as a result of the updated inventory. As discussed in Section 5.5.1, the solid source term for the PABC-2009 inventory is lower after roughly 350 years and remains lower for the rest of the 10,000-year regulatory period. As a result, the direct solid releases from spallings decreased. The rank regression analysis indicates that the dominant parameters with regard to controlling spallings releases in the PABC-2009 are the intact halite porosity and the particle diameter for disaggregated waste (Kirchner 2010b).

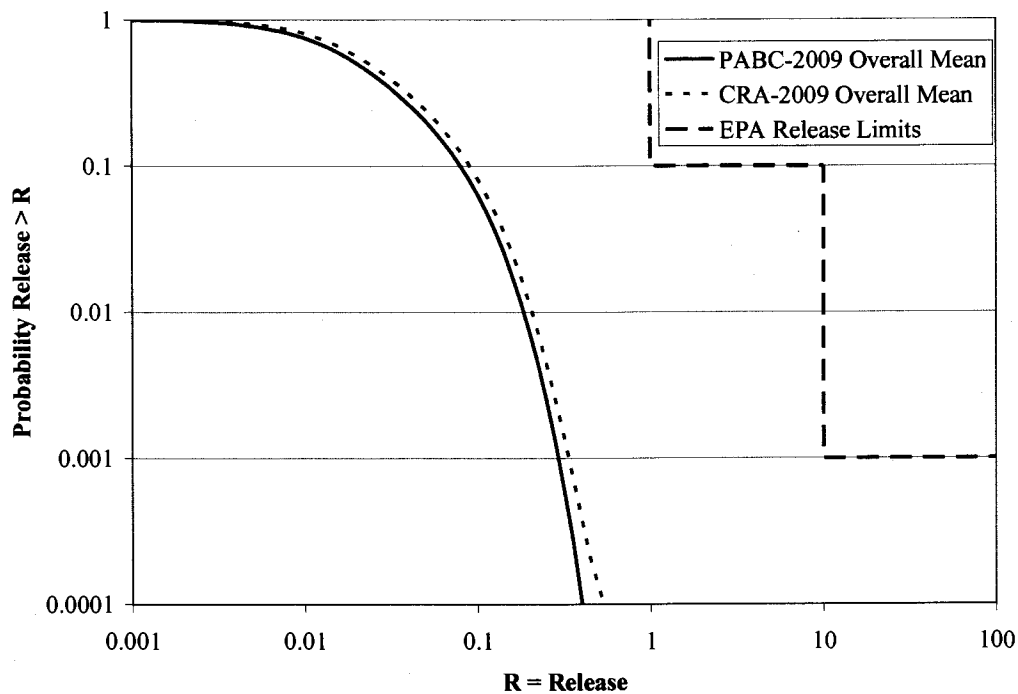


Figure 6-1. Overall mean CCDFs for cuttings and cavings releases in EPA units, PABC-2009 and CRA-2009 PA.

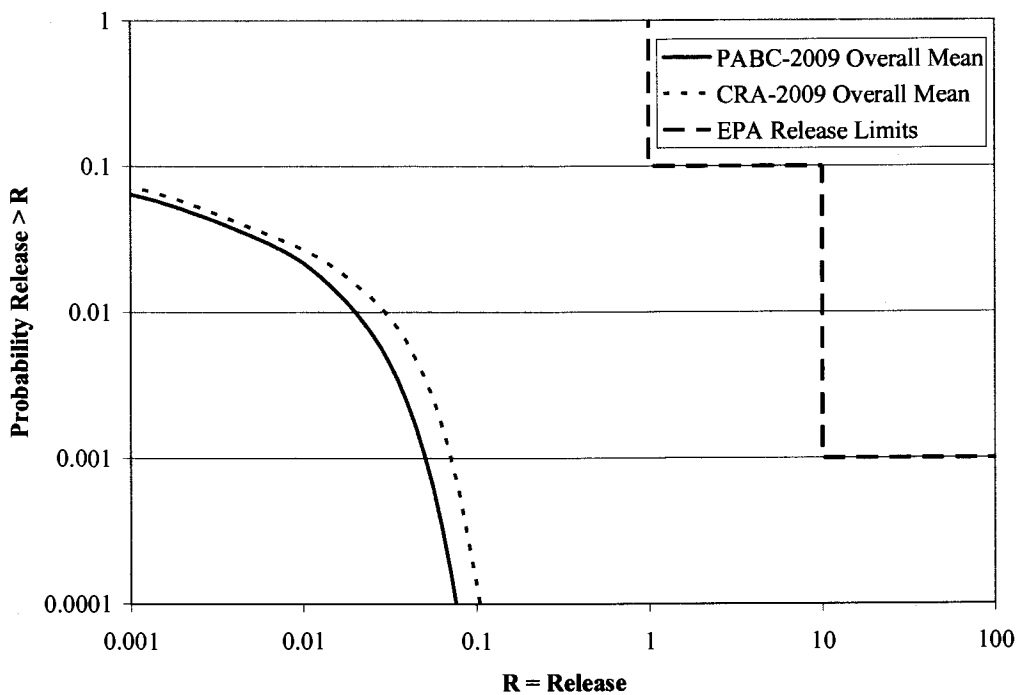


Figure 6-2. Overall mean CCDFs for spallings releases in EPA units, PABC-2009 and CRA-2009 PA.

6.3 DIRECT BRINE RELEASES

The overall mean CCDFs for DBRs from the PABC-2009 and the CRA-2009 PA are shown in Figure 6-3. An increase in the PABC-2009 compared with the CRA-2009 PA is observed and two knees in the curve are present in the PABC-2009 that were not present in the CRA-2009 PA. DBR volumes to the surface were very similar in both analyses, resulting in overall volume CCDFs that were nearly identical (Camphouse 2010). Therefore, the increase in overall mean CCDF for DBR was caused by the increase in the actinide concentrations in the brine. Higher radionuclide solubility limits resulted in an increase in total mobilized concentration, increasing the release associated with a given brine volume.

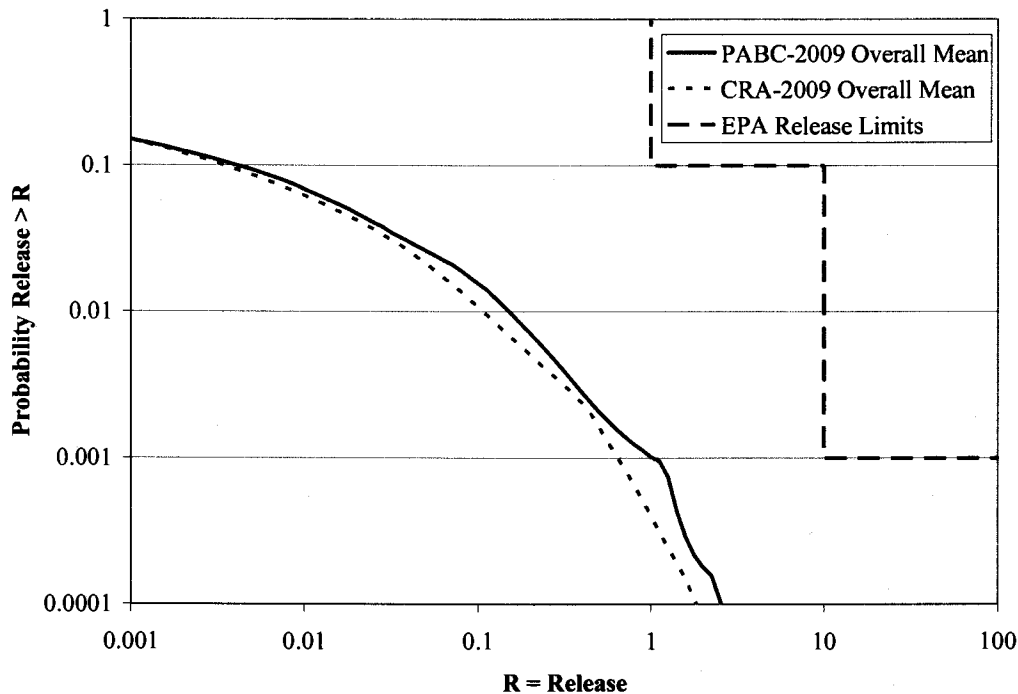


Figure 6-3. Overall mean CCDFs for DBRs in EPA units, PABC-2009 and CRA-2009 PA.

The rank regression analysis shows that four variables, the “solubility multiplier” that represents uncertainty in solubility limits for all actinides in the III oxidation state (Xiong et al. 2009), the initial brine pore pressure in the Castile Formation, the frequency with which Castile brine intrudes the repository due to a drilling event and the inundated corrosion rate for steel, account for more than 50% of the uncertainty in DBRs for the PABC-2009 (Kirchner 2010b). These variables are also important in the CRA-2009 PA analysis although the third- and fourth-ranked variables are in reverse order relative to the PABC-2009 (Kirchner 2010b). The solubility of actinides impacts their concentration in the DBRs. An increase in the solubility limit increases the concentration of actinides in the brine. The frequency with which Castile brine intrudes the repository due to a drilling event and the initial pressure of that brine affect the pressure in the repository. As DBR volumes are a strong function of pressure, a positive correlation is expected and shown (Kirchner 2010b).

6.4 GROUNDWATER TRANSPORT

Figure 6-4 shows the overall mean CCDF for normalized releases from the Culebra for the PABC-2009 and the mean CCDF for replicate R2 of the CRA-2009 PA. Since, no transport releases larger than 10^{-6} EPA units occurred in replicates R1 and R3 of the CRA-2009 PA, calculating the overall mean CCDF for the CRA-2009 PA was problematic. Normalized transport releases for the PABC-2009 are much higher compared with the CRA-2009 PA. The overall mean for the PABC-2009 is approximately two orders of magnitude larger than the mean of replicate R2 from the CRA-2009 PA. Instead of only one replicate exhibiting releases that are significantly larger than the numerical error inherent in the transport calculations, all three replicates in the PABC-2009 show appreciable normalized releases from the Culebra. This increase is mainly due to the increase in the transport through the Culebra (see Section 5.4.5) while the increase of transport through the borehole (see Section 5.4.4) also contributed (Camphouse 2010). The rank regression analysis indicates that the dominant parameters with regard to controlling releases from the Culebra in the PABC-2009 are the borehole permeability and the matrix partition coefficient for uranium (Kirchner 2010b).

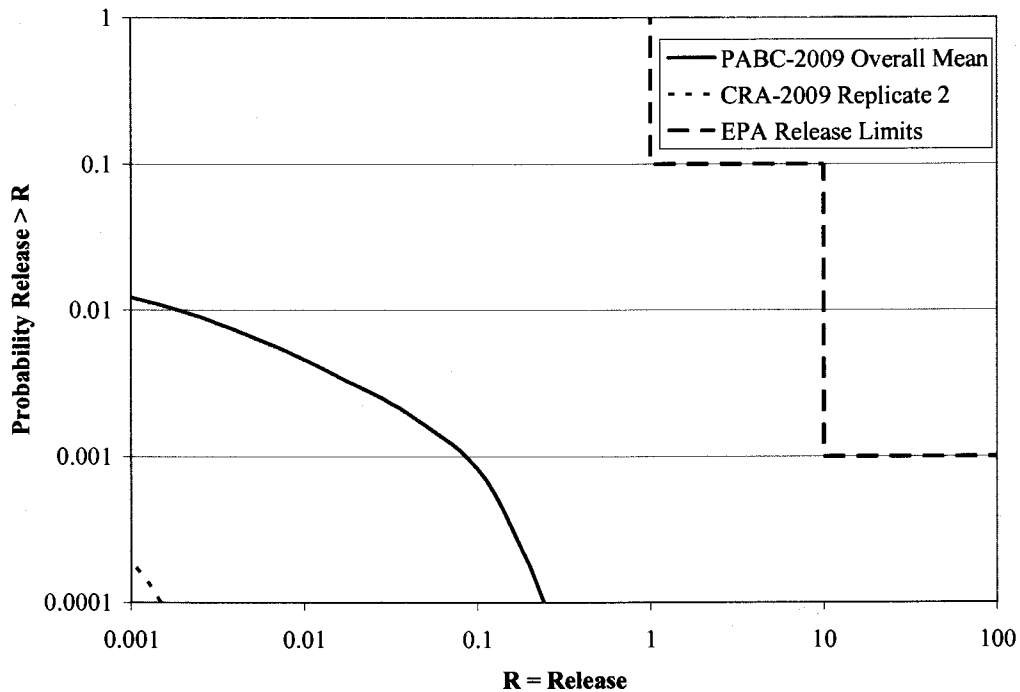


Figure 6-4. Mean CCDFs for releases from the Culebra in EPA units, PABC-2009 and CRA-2009 PA.

6.5 TOTAL

Total releases are calculated by totaling the releases from each release pathway: cuttings and cavings releases, spallings releases, DBRs, and transport releases (there were no undisturbed releases to contribute to the total release). To quantitatively determine the sufficiency of the sample size, a confidence interval is computed about the overall mean CCDF using the Student's t-distribution and the mean CCDFs from each replicate. Figure 6-5 shows 95 percent confidence

intervals about the overall mean for total releases. The CCDF and confidence intervals lie below and to the left of the limits specified in 40 CFR § 191.13(a). Thus, the WIPP continues to comply with the containment requirements of 40 CFR Part 191.

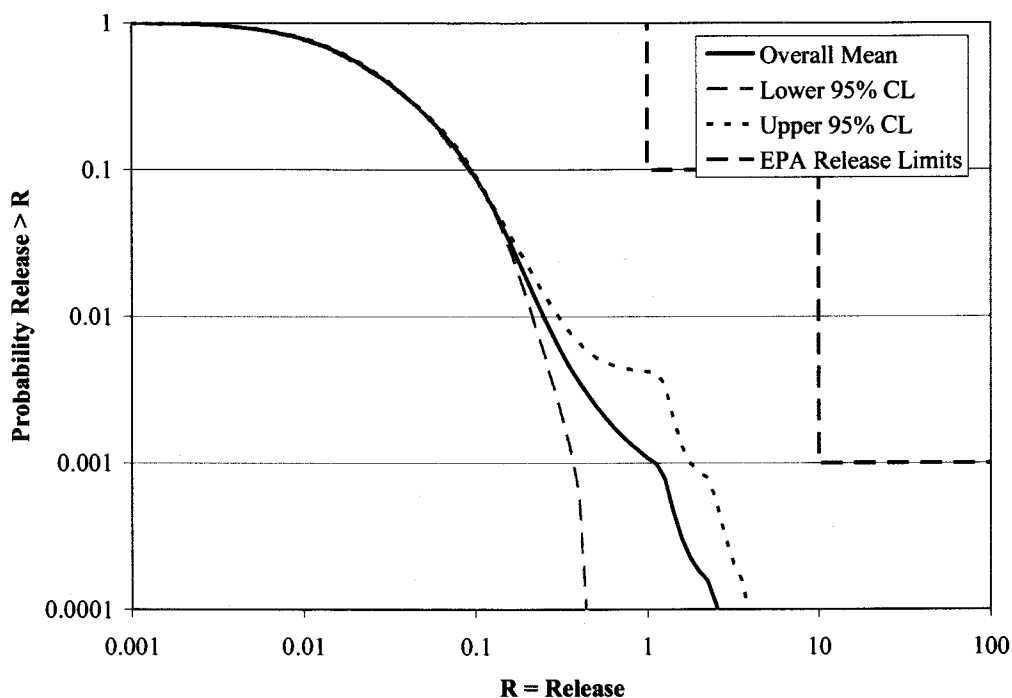


Figure 6-5. Confidence interval on overall mean CCDF for total normalized releases in EPA units, PABC-2009.

Figure 6-6 shows the 300 CCDFs from replicates R1, R2 and R3 of the PABC-2009, used to calculate the overall mean and confidence intervals (Camphouse 2010). As seen in Figure 6-6, one vector generated a CCDF considerably different than the other 299. However, this does not result in the WIPP being out of compliance with the containment requirements. As set forth in the Certification Criteria in Title 40 CFR Part 194, compliance is specified on the overall mean and its lower/upper 95% confidence limits, not the individual vectors (U.S. EPA 1998, Section VIII.B.5.b). The DBR dominates the total release in the outlier CCDF (Camphouse 2010), which increased due to the increase in total mobilized concentration (see Section 6.3).

Cuttings, cavings and DBRs account for the majority of the total releases estimated in the PABC-2009. Figure 6-7 shows the overall mean CCDFs for each component of total releases for the PABC-2009. The considerable increase for releases from the Culebra was not large enough to influence the total releases, although releases from the Culebra are now on the same order as releases due to spillings (Camphouse 2010).

As indicated in the rank regression analysis, uncertainty in total normalized releases is largely due to uncertainty in waste shear strength (Kirchner 2010b). The volumes of cuttings and cavings are primarily controlled by shear strength (Ismail 2010). The “solubility multiplier” which represents uncertainty in solubilities for all actinides in the III oxidation state (Xiong et al. 2009) and initial brine pore pressure in the Castile Formation also contribute to variability in

total releases in all replicates (Kirchner 2010b). Solubility of actinides impacts their concentration in DBRs and the brine pressure in the Castile Formation affects the DBR volumes.

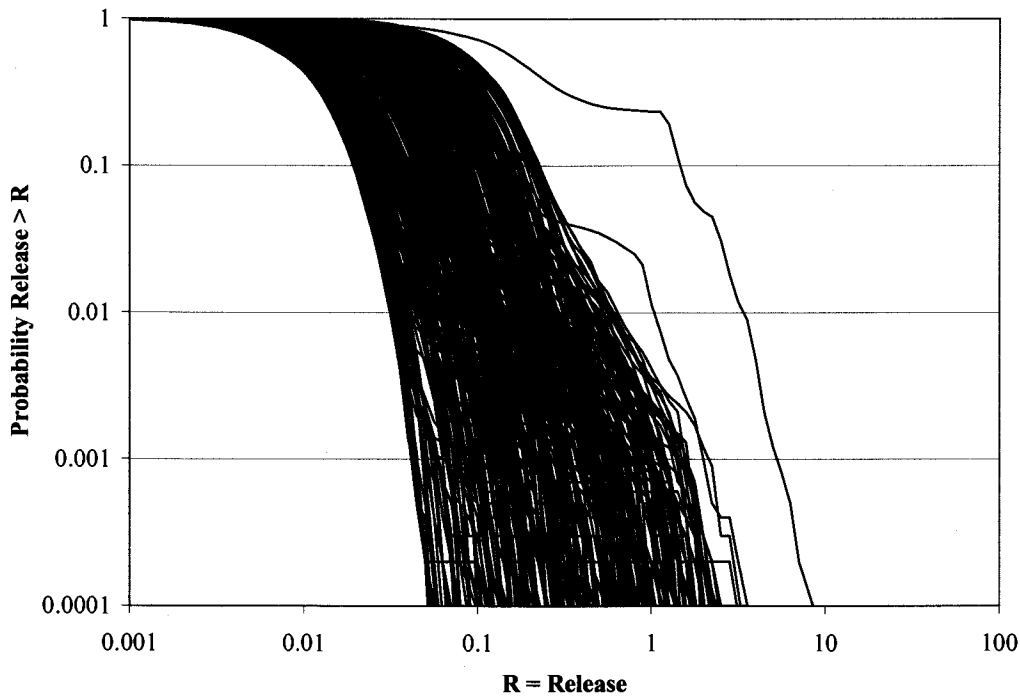


Figure 6-6. Total normalized releases in EPA units, replicates R1, R2 and R3, PABC-2009.

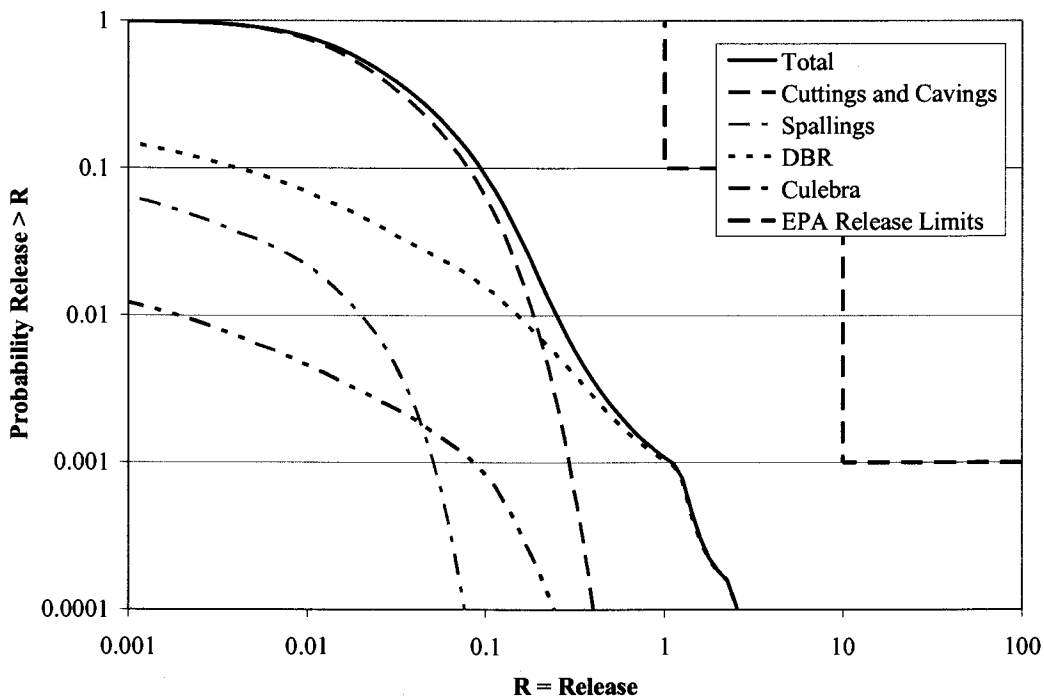


Figure 6-7. Overall mean CCDFs for components of total normalized releases in EPA units, PABC-2009.

Figure 6-8 provides a comparison between the overall mean CCDFs for total releases for the PABC-2009 and the CRA-2009 PA. At high probabilities, the overall mean CCDF for total normalized releases is lower for the PABC-2009, while at low probabilities it is higher for the PABC-2009 (Camphouse 2010). The decrease at high probabilities is due to the decrease in the cutting and cavings (see Section 6.1), while the increase at low probabilities is because of the increase of DBRs (see Section 6.3). Mean total releases differ by ~0.01 EPA units at a probability of 0.1 and ~0.4 EPA units at a probability of 0.001 (Table 6-1).

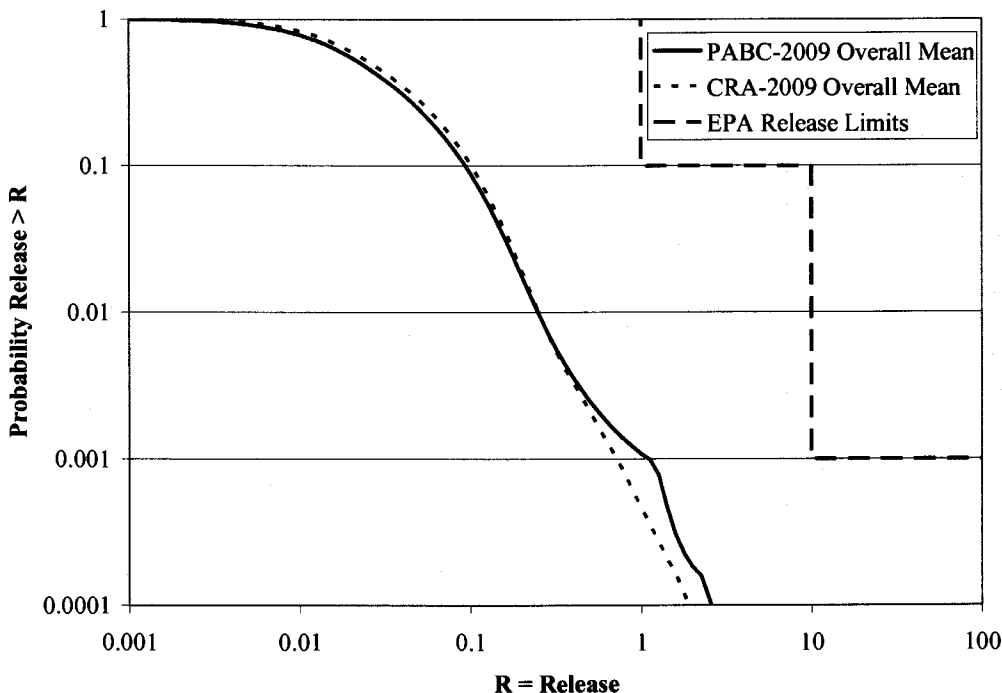


Figure 6-8. Overall mean CCDFs for total normalized releases in EPA units, PABC-2009 and CRA-2009 PA.

Table 6-1. PABC-2009 and CRA-2009 PA statistics on the overall mean for total normalized releases in EPA units at probabilities of 0.1 and 0.001.

Probability	Analysis	Mean Total Release	90 th Percentile	Lower 95% CL	Upper 95% CL	Release Limit
0.1	CRA-2009 PA	0.10	0.17	0.10	0.11	1
	PABC-2009	0.09	0.16	0.09	0.10	1
0.001	CRA-2009 PA	0.72	0.81	0.48	0.92	10
	PABC-2009	1.10	1.00	0.37	1.77	10

There are some definite similarities between the CCDFs for the two analyses. First, cuttings and cavings and DBRs are the most significant pathways for release of radioactive material to the land surface. Second, release by spillings and subsurface transport in the Salado or Culebra make essentially no contribution to total releases. Finally, the resulting CCDFs of both analyses are within regulatory limits.

REFERENCES

- Beauheim, R.L. 2009. Culebra and Magenta Pressure and Permeability Values for Use in BRAGFLO. Sandia National Laboratories, Carlsbad, NM. ERMS 551646.
- Burgess, A., T. Doe and T. Lowenstein. 2008. Culebra Hydrogeology Conceptual Model Peer Review, Final Report, September 24, 2008. Report for the Carlsbad Field Office Technical Assistance Contractor in Support of the U.S. Department of Energy.
- Brush, L.H. and L.J. Storz 1996. Revised Ranges and Probability Distributions of Kds for Dissolved Pu, Am, U, Th and Np in the Culebra for the PA Calculations to Support the WIPP CCA. Memorandum to M.S. Tierney, Sandia National Laboratories, Albuquerque, NM. ERMS 241561.
- Brush, L.H., Y. Xiong and J.J. Long. 2009. Results of the Calculation of Actinide Solubilities for the WIPP CRA-2009 PABC. Sandia National Laboratories, Carlsbad, NM. ERMS 552201.
- Camphouse, R.C. 2010. Analysis Package for CCDFGF: CRA-2009 Performance Assessment Baseline Calculation. Sandia National Laboratories, Carlsbad, NM. ERMS 553027.
- Chavez, M. 2009. SNL WIPP Surveillance IS-09-12 Report for PABC-2009 Input Files, Revision 0. Sandia National Laboratories, Carlsbad, NM. ERMS 552230.
- Clayton, D.J. 2009a. Analysis Plan for the CRA-2009 Performance Assessment Baseline Calculation. Sandia National Laboratories, Carlsbad, NM. ERMS 551603.
- Clayton, D.J. 2009b. Corrections to and Reduction from Fifteen to Three for the Direct Brine Release PREBRAG Input Files. Sandia National Laboratories, Carlsbad, NM. ERMS 551944.
- Clayton, D.J. 2009c. Modification to PANEL Calculation Sequence to Include Automatic Calculation of the LSOLDIFF Values. Sandia National Laboratories, Carlsbad, NM. ERMS 551947.
- Clayton, D.J. 2009d. New Parameters Needed for the PABC-2009 DBR Calculations. Sandia National Laboratories, Carlsbad, NM. ERMS 551715.
- Clayton, D.J. 2009e. Update to K_d Values for the PABC-2009. Sandia National Laboratories, Carlsbad, NM. ERMS 552395.
- Clayton, D.J. 2010a. Analysis Package for Direct Brine Releases: CRA-2009 Performance Assessment Baseline Calculation. Sandia National Laboratories, Carlsbad, NM. ERMS 552829.
- Clayton, D.J. 2010b. Parameter Summary Report: CRA-2009 Performance Assessment Baseline Calculation. Sandia National Laboratories, Carlsbad, NM. ERMS 552889.

Summary Report of the CRA-2009 Performance Assessment Baseline Calculation

- Clayton, D.J., S. Dunagan, J.W. Garner, A.E. Ismail, T.B. Kirchner, G.R. Kirkes, M.B. Nemer. 2008. Summary Report of the 2009 Compliance Recertification Application Performance Assessment. Sandia National Laboratories, Carlsbad, NM. ERMS 548862.
- Cotsworth, E. 2005. EPA Letter on Conducting the Performance Assessment Baseline Change (PABC) Verification Test. U.S. EPA, Office of Radiation and Indoor Air, Washington, D.C. ERMS 538858.
- Cotsworth, E. 2009. EPA Letter on CRA-2009 First Set of Completeness Comments. U.S. EPA, Office of Radiation and Indoor Air, Washington, D.C. ERMS 551444.
- Crawford, B., D. Guerin, S. Lott, B. McInroy, J. McTaggart, G. Van Soest. 2009. Performance Assessment Inventory Report – 2008. Los Alamos National Laboratory, Carlsbad, NM. LA-UR-09-02260. ERMS 551511.
- Fox, B. and D.J. Clayton 2010. Analysis Package for EPA Unit Loading Calculations: CRA-2009 Performance Assessment Baseline Calculation. Sandia National Laboratories, Carlsbad, NM. ERMS 552912.
- Fox, B., D.J. Clayton, T.B. Kirchner. 2009. Radionuclide Inventory Screening Analysis Report for the PABC-2009. Sandia National Laboratories, Carlsbad, NM. ERMS 551679.
- Garner, J.W. 2006. Software Installation and Checkout and Regression Testing Report of PANEL, Version 4.03 on the Compaq ES40, ES45 and ES47 Platforms Using OpenVMS 8.2. Sandia National Laboratories, Carlsbad, NM. ERMS 543600.
- Garner, J.W. 2010. Analysis Package for PANEL: CRA-2009 Performance Assessment Baseline Calculation. Sandia National Laboratories, Carlsbad, NM. ERMS 553032.
- Gilkey, A.P. 2006. Software Installation and Checkout and Regression Testing Report of NUTS Version 2.05c on the Compaq ES40, ES45 and ES47 Platforms. Sandia National Laboratories, Carlsbad, NM. ERMS 543789.
- Ismail, A.E. 2010. Analysis Package for Cuttings, Cavings, and Spallings: CRA-2009 Performance Assessment Baseline Calculation. Sandia National Laboratories, Carlsbad, NM. ERMS 552893.
- Ismail, A.E. and J.W. Garner. 2008. Analysis Package for Salado Transport Calculations: Compliance Recertification Application 2009. Sandia National Laboratories, Carlsbad, NM. ERMS 548845.
- Ismail, A.E. and J.W. Garner. 2010. Analysis Package for Salado Transport Calculations: CRA-2009 Performance Assessment Baseline Calculation. Sandia National Laboratories, Carlsbad, NM. ERMS 552943.
- Kanney, J.F. 2006. Software Installation and Checkout and Regression Testing Report of SECOTP2D, Version 1.41A on the Compaq ES40, ES45 and ES47 Platforms Using OpenVMS 8.2. Sandia National Laboratories, Carlsbad, NM. ERMS 543596.

Summary Report of the CRA-2009 Performance Assessment Baseline Calculation

- Kelly, T.E. 2009. EPA Third Letter Requesting Additional Information on the CRA-2009. U.S. EPA, Office of Radiation and Indoor Air, Washington, D.C. ERMS 552374.
- Kirchner, T.B. 2006. Software Installation and Checkout and Regression Testing Report of STEPWISE Version 2.21 on the Compaq ES40, ES45 and ES47 Platforms Using OpenVMS 8.2. Sandia National Laboratories, Carlsbad, NM. ERMS 543589.
- Kirchner, T.B. 2010a. Generation of the LHS Samples for the AP-145 (PABC09) PA Calculations. Sandia National Laboratories, Carlsbad, NM. ERMS 552905.
- Kirchner, T.B. 2010b. Sensitivity of the CRA-2009 Performance Assessment Baseline Calculation Releases to Parameters. Sandia National Laboratories, Carlsbad, NM. ERMS 552960.
- Kirkes, G.R. 2009a. Baseline Features, Events, and Processes List for the Waste Isolation Pilot Plant, Revision 2. Sandia National Laboratories, Carlsbad, NM. ERMS 551874.
- Kirkes, G.R. 2009b. Features, Events and Processes Assessment for Changes Described in Analysis Plan - 145. Sandia National Laboratories, Carlsbad, NM. ERMS 551888.
- Kirkes, G.R. 2009c. Procedure SP 9-4, Revision 2, Performing FEPs Baseline Impact Assessments for Planned or Unplanned Changes. Sandia National Laboratories, Carlsbad, NM. ERMS 551859.
- Kuhlman, K.L. 2010. Analysis Report for the CRA-2009 PABC Culebra Flow and Transport Calculations. Sandia National Laboratories, Carlsbad, NM. ERMS 552951.
- Leigh, C.D. 2006. Software Installation and Checkout and Regression Testing Report of EPAUNI, Version 1.15A on the Compaq ES40, ES45 and ES47 Platforms Using OpenVMS 8.2. Sandia National Laboratories, Carlsbad, NM. ERMS 543779.
- Leigh, C.D., J.F. Kanney, L.H. Brush, J.W. Garner, G.R. Kirkes, T. Lowry, M.B. Nemer, J.S. Stein, E.D. Vugrin, S. Wagner, and T.B. Kirchner. 2005. 2004 Compliance Recertification Application Performance Assessment Baseline Calculation, Revision 0. Sandia National Laboratories, Carlsbad, NM. ERMS 541521.
- Long, J.J. 2010. Execution of Performance Assessment Codes for the CRA-2009 Performance Assessment Baseline Calculation. Sandia National Laboratories, Carlsbad, NM. ERMS 552947.
- MacKinnon, R.J., and G. Freeze. 1997a. Summary of EPA-Mandated Performance Assessment Verification Test (Replicate 1) and Comparison with the Compliance Certification Application Calculations, Revision 1. Sandia National Laboratories, Carlsbad, NM. ERMS 422595.
- MacKinnon, R.J., and G. Freeze. 1997b. Summary of Uncertainty and Sensitivity Analysis Results for the EPA-Mandated Performance Assessment Verification Test, Rev. 1. Sandia National Laboratories, Carlsbad, NM. ERMS 420669.

Summary Report of the CRA-2009 Performance Assessment Baseline Calculation

- MacKinnon, R.J., and G. Freeze. 1997c. Supplemental Summary of EPA-Mandated Performance Assessment Verification Test (All Replicates) and Comparison with the Compliance Certification Application Calculations, Revision 1. Sandia National Laboratories, Carlsbad, NM. ERMS 414880.
- McKenna, S.A. and M.J. Chavez. 2005. Software Installation and Checkout for MODFLOW 2000, Version 1.6. Sandia National Laboratories, Carlsbad, NM. ERMS 540470.
- Nemer, M.B. 2007. Software Installation and Checkout for BRAGFLO, Version 6.0. Sandia National Laboratories, Carlsbad, NM. ERMS 545019.
- Nemer, M.B. 2009. New Parameters, Removal of Hard Coded Values, and Checking of BRAGFLO Input Files for the PABC-2009. Sandia National Laboratories, Carlsbad, NM. ERMS 551710.
- Nemer, M.B. 2010. Analysis Package for Salado Flow Modeling: CRA-2009 Performance Assessment Baseline Calculation. Sandia National Laboratories, Carlsbad, NM. ERMS 552956.
- U.S. Department of Energy (DOE) 1996. Title 40 CFR Part 191 Compliance Certification Application for the Waste Isolation Pilot. U.S. Department of Energy Waste Isolation Pilot Plant, Carlsbad Area Office, Carlsbad, NM. DOE/CAO-1996-2184.
- U.S. Department of Energy (DOE) 2004. Title 40 CFR Part 191 Compliance Recertification Application for the Waste Isolation Pilot Plant, , 10 vols., U.S. Department of Energy Waste Isolation Pilot Plant, Carlsbad Field Office, Carlsbad, NM. DOE/WIPP 2004-3231.
- U.S. Department of Energy (DOE). 2007. Delaware Basin Monitoring Annual Report. U.S. Department of Energy Waste Isolation Pilot Plant, Carlsbad Area Office, Carlsbad, NM. DOE/WIPP-07-2308.
- U.S. Department of Energy (DOE). 2008. Delaware Basin Monitoring Annual Report. U.S. Department of Energy Waste Isolation Pilot Plant, Carlsbad Area Office, Carlsbad, NM. DOE/WIPP-08-2308.
- U.S. Environmental Protection Agency (EPA). 1993. 40 CFR Part 191: Environmental Radiation Protection Standards for the Management and Disposal of Spent Nuclear Fuel, High-Level and Transuranic Radioactive Wastes; Final Rule. Federal Register, Vol. 58, 66398-66416.
- U.S. Environmental Protection Agency (EPA). 1996. 40 CFR Part 194: Criteria for the Certification and Recertification of the Waste Isolation Pilot Plant's Compliance with the 40 CFR Part 191 Disposal Regulations; Final Rule. Federal Register, Vol. 61, 5223-5245.
- U.S. Environmental Protection Agency (EPA). 1998. 40 CFR 194, Criteria for the Certification and Recertification of the Waste Isolation Pilot Plant's Compliance with the Disposal Regulations: Certification Decision: Final Rule, Federal Register. Vol. 63, 27354-27406. ERMS 251924.

Summary Report of the CRA-2009 Performance Assessment Baseline Calculation

- Vugrin, E.D. 2005. Analysis Package for DRSPALL, CRA 2004 Performance Assessment Baseline Calculation. Sandia National Laboratories, Carlsbad, NM. ERMS 540415.
- Vugrin, E.D. 2006a. Software Installation and Checkout and Regression Testing for CUTTINGS_S, Version 6.02 on the Compaq ES40, ES45 and ES47 Platforms Using OpenVMS 8.2. Sandia National Laboratories, Carlsbad, NM. ERMS 537042.
- Vugrin, E.D. 2006b. Software Installation and Checkout and Regression Testing Report of DRSPALL, Version 1.10 on the Compaq ES40, ES45 and ES47 Platforms Using OpenVMS 8.2. Sandia National Laboratories, Carlsbad, NM. ERMS 543773.
- Vugrin, E.D. 2006c. Software Installation and Checkout and Regression Testing Report of CCDFGF, Version 5.02 on the Compaq ES40, ES45 and ES47 Platforms Using OpenVMS 8.2. Sandia National Laboratories, Carlsbad, NM. ERMS 543452.
- Vugrin, E.D. 2006d. Software Installation and Checkout and Regression Testing Report of LHS, Version 2.42 on the Compaq ES40, ES45 and ES47 Platforms Using OpenVMS 8.2. Sandia National Laboratories, Carlsbad, NM. ERMS 543786.
- Xiong, Y., L.H. Brush, A.E. Ismail and J.J. Long. 2009. Uncertainty Analysis of Actinide Solubilities for the WIPP CRA-2009 PABC. Sandia National Laboratories, Carlsbad, NM. ERMS 552500.

Trone, Janis R

From: Chavez, Mario Joseph
Sent: Wednesday, February 10, 2010 5:57 PM
To: Trone, Janis R
Cc: Clayton, Daniel James
Subject: Signature Authority

Handwritten signature and date: 2/10/10

Janis,

If needed, I give you permission to sign for me as the QA Reviewer for the "Summary Report of the CRA-2009 Performance Assessment Baseline Calculation". All my comments have been resolved and the DRC is all signed off.

Thanks,

Mario

Clayton, Daniel James

From: Ismail, Ahmed
Sent: Wednesday, February 10, 2010 9:46 AM
To: Clayton, Daniel James
Subject: RE: PABC09 Summary Report



Hi, Dan:

Things have been, well, interesting here in CT. (Snowmageddon Part II is currently underway.)

I hereby give Dan Clayton my signature authority for the PABC Summary Report and any related documents.

--AEI

=====
Ahmed E. Ismail
Sandia National Labs
NHPA/502 || MS 1395 || 505-844-1313
aismail@sandia.gov<mailto:aismail@sandia.gov>

From: Clayton, Daniel James
Sent: Wednesday, February 10, 2010 9:34 AM
To: Ismail, Ahmed
Subject: PABC09 Summary Report

Ahmed,

Hope you are having fun. We are signing the summary report. Can you send me signature authority?

Thanks,
Dan